

AD-A198 614

2010-PA

2

AD

DEVELOPMENT OF HIGH MOBILITY SEMICONDUCTOR SYSTEMS AND DEVICES
FOR DIMENSIONAL EFFECTS AND TUNING

DEVELOPMENT OF HIGH MOBILITY SEMICONDUCTOR SYSTEMS AND DEVICES
FOR DIMENSIONAL EFFECTS AND TUNING

DEVELOPMENT OF HIGH MOBILITY SEMICONDUCTOR SYSTEMS AND DEVICES
FOR DIMENSIONAL EFFECTS AND TUNING

DEVELOPMENT OF HIGH MOBILITY SEMICONDUCTOR SYSTEMS AND DEVICES
FOR DIMENSIONAL EFFECTS AND TUNING

DTIC
SELECTED
AUG 11 1981
S E D

United States Army
EUROPEAN RESEARCH OFFICE FOR THE U.S. ARMY
London, England

CONTRACT NUMBER - DAA1981-1-0001

USACE

This document has been approved
for release and sale in
unlimited quantities.

ADA198614

Unidentified

The parameters measured here will be of direct application in study of high T_c superconductor interactions with silicon substrates.

Part II describes similar measurements on defects in GaAs. Defects in this compound semiconductor are much more difficult to characterize, primarily because the best technology--electron spin resonance--is not so widely applicable as in Si; thus the electrical data cannot be clearly associated with specific point defect structures. This work is being continued with attention to unusual ESR-related techniques in hopes of a definitive identification and modeling of the defects so far observed.

Part III presents initial work in ESR studies of high T_c superconductors. It is essential to develop a picture of paramagnetic behaviour within the body of the superconductor before proceeding to the planned examination of transferred superconductor influence on defects and carriers in an underlying semiconductor substrate. This work is also being continued.

FINAL REPORT

23 May 1988

DEFECTS IN HIGH-MOBILITY SEMICONDUCTOR SYSTEMS

Contract: DAJA45-87-C-0052 R&D Proposal: 5919-PH-01

Experimental work funded under the subject contract was completed at the University of Lund during the period 23 Dec 1987-23 April 1988. The observed findings have now been assessed and interpreted, and the results are presented here in 3 parts.

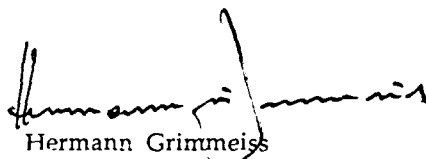
Part I describes research on the P_b center of oxidized silicon surfaces. This center provided an important test defect for inauguration of a new opto-electronic measurement system which was assembled at Fort Monmouth as part of the planned research. The P_b center is the most important defect in MOS integrated circuit technology. In addition to being of much interest in itself, it provides an excellent probe to test interface interactions with current carrier holes and electrons, and with overlying layers of other semiconductors or superconductors. The optical absorption thresholds of this center were determined by the initial slope method, and compared with electrical energies to yield the Franck-Condon configurational change--found to be in good accord with molecular orbital theory. The parameters measured here will be of direct application in study of high- T_c superconductor interactions with silicon substrates.

Part II describes similar measurements on defects in GaAs. Defects in this compound semiconductor are much more difficult to characterize, primarily because the best technology--electron spin resonance-- is not so widely applicable as in Si; thus the electrical data cannot be clearly associated with specific point defect structures. This work is being continued with attention to unusual ESR-related techniques in hopes of a definitive identification and modeling of the defects so far observed (no added support is required, as per original proposal).

Part III presents initial work in ESR studies of high- T_c superconductors. It is essential to develop a picture of paramagnetic behavior within the body of the superconductor before proceeding to the planned examination of transferred superconductor influence on defects and carriers in an underlying semiconductor substrates. This work is also being continued without additional funding support, as noted above.

Accession For	
NTIS GRA&I	<input checked="" type="checkbox"/>
DTIC TAB	<input type="checkbox"/>
Unannounced	<input type="checkbox"/>
Justification	
By _____	
Distribution/	
Availability Codes	
Dist	Avail and/or Special
A-1	




Hermann Grimmer
Principal Investigator
Department of Solid State Physics
University of Lund

RESEARCH REPORT

PART I

**Optical and Electrical Studies of Interface Traps in the Si/SiO₂ System by
Modified Junction Space Charge Techniques**

I. Introduction

Understanding of interface defects in Si/SiO₂ structures has improved significantly during the past few years, primarily due to electron spin resonance (ESR). Realistic structural models for several important defects have been determined, with special emphasis on trivalent silicon defects at the interface, termed P_b centers.^(1,2) Quantitative correlation of physical, chemical, and electrical properties indicate that P_b centers are the defect source of about half of the interface states.⁽³⁾ However, study of detailed electrical and optical properties of P_b centers is far from complete, and there are still numerous uncertainties regarding the electronic properties of all interface states throughout the bandgap.

Over the same time span, there have also been important advances in the electrical and optical characterization of bulk traps in Si, especially by use of junction space charge techniques.^(4,5) These have contributed to considerable improvement in the understanding of the electronic properties of bulk defects. In the present work, we have applied some of these techniques, slightly modified for the metal-oxide-silicon (MOS) test structure, to learn more about the electronic properties of interface traps. The application of modified junction space charge techniques to MOS systems has several advantages, but is not entirely unprecedented. A brief comparison of the junction and MOS methods for trap study has been given by Nicollian and Brews.⁽⁶⁾ In corollary, bulk traps have been studied with the MOS technique by careful ion implantation.⁽⁷⁾ An important advantage of MOS test samples is the lack of current flow, which on the one hand somewhat simplifies the application of junction techniques to the MOS case, but on the other, implies some complication which will be briefly discussed later.

The apparent spectrum of interface trap levels within the forbidden energy gap is a rather featureless U-shaped continuum when the total density of traps is low. However, with higher densities, richer structure has been observed by several investigators, including peaks at various energies.⁽⁸⁾ Most recently, with trap densities $\geq 10^{12}$ cm⁻² on (111) Si, two peaks are found at 0.3eV and 0.85eV above the valence band, superimposed on a U-shaped background. These peaks were first clearly observed with deep level transient spectroscopy (DLTS)⁽⁹⁾ and later quantitatively correlated with similar peaks from electric-field-controlled ESR.⁽¹⁰⁾ Other groups have also examined the nature and bandgap distribution of interface traps by ESR and capacitance-voltage (C-V) analysis.⁽¹¹⁻¹³⁾

Optical properties of uncharacterized interface traps in the Si/SiO₂ structure have been examined several times previously.⁽¹⁴⁻¹⁶⁾ The general approach has been

the use of subband-gap monochromatic light to induce electronic transitions between the localized states of interface defects and the extended states of silicon. These transitions were detected by monitoring either photocurrent or photocapacitance transients in MOS devices. Data analysis yielded interface-state distributions and photoionization cross sections. However, the above optical studies were conducted without knowledge of P_b -centers, and usually on fully-processed MOS devices which did not have identifiable P_b concentrations.

A number of optical studies of limited scope have been specifically directed to P_b centers. In a recent study, optical absorption by P_b centers was measured by electroabsorption spectroscopy with subband-gap monochromatic light on MOS capacitors.⁽¹⁷⁾ The results yielded an interface-state distribution with a band of states centered near $E_v + 0.3$ eV. The study also concluded that optical absorption by singly-occupied P_b centers is dominated by hole emission, in contrast to the dangling bond defect in amorphous silicon where electron photoemission dominates.⁽¹⁸⁾ With photothermal deflection spectroscopy, it has also been determined that the optical cross section for electron emission from the singly-occupied P_b center is small (i.e., $< 10^{-17}$ cm²).⁽¹⁹⁾ P_b centers have also been detected by optically-induced spin-dependent recombination⁽²⁰⁾ and by optically-detected magnetic resonance⁽²¹⁾, although these studies did not establish the distribution or optical properties of the deep levels. Finally, limited results are available from photocurrent transient spectroscopy, which reveal substantial photoionization of P_b centers with 0.37 eV photons⁽²²⁾.

The present study extends these earlier measurements with more comprehensive data on the optical and electrical properties of P_b centers as measured by modified junction space charge techniques. Photoionization spectra and thresholds for holes and electrons in interface traps have been determined, as well as absolute values for optical cross sections by use of photocapacitance, which is much more sensitive than the usual ESR approaches. Single-shot electrical methods, including pulse train techniques, and DLTS measurements have been used to examine carrier capture and thermal emission processes. The analysis of the investigations was greatly simplified since most of the optical and thermal capacitance transients were exponential. It was therefore possible to measure the enthalpies of interface traps in both n- and p-type samples.

II. Experimental Techniques

All measurements here were performed on MOS capacitors fabricated on (111) oriented Czochralski silicon, p- and n-type, $\geq 30\Omega\text{cm}$. The samples were selected from

those remaining from previous studies,^(2,9) in order to improve correlation of results. The samples had been oxidized in such a way as to achieve a high density D_{it} of interface traps in general and P_b centers in particular. A typical sample is shown in Fig. 1; the small Al dots are for electrical or optical measurements; the large Al capacitor is for gated ESR.

The optical experiments were performed in a liquid-N₂ cryostat with optical windows. A Kratos single-grating monochromator with a 1000 watt tungsten lamp, in conjunction with suitable filters, was used as a light source. Spectral distributions were measured with a vacuum double grating monochromator. Most of the spectral distributions were studied employing the initial slope technique⁽²³⁾ in measuring the change in the capacitance due to the illumination with monochromatic light. The intensities were chosen such that the response times were of the order of seconds.

All electrical measurements were performed in a commercial DLTS equipment from Polaron; this equipment served for single-shot measurements, for pulse-train capture studies, and of course, for DLTS. Supporting ESR measurements were made on Varian E-line Century x-band spectrometers.

Additional details on samples and experimental techniques are given in the references cited or in the appropriate sections to follow.

III. Experimental Results

A. Preliminary Characterization

The samples used for this study were given a preliminary examination by G-V and capacitance voltage (C-V) analysis at 300K, to establish the broad features of the traps present. High frequency (1MHz) and low-frequency (10Hz) C-V and G-V curves for a p-type sample are shown in Fig. 2; other p-type samples and n-type samples were very similar. The G-V curves show a large peak in the depletion region, overshadowing losses elsewhere, and demonstrate the dominance of interface traps, as opposed to bulk traps. The bandgap energy level spectrum of interface traps is shown in Fig. 3; the results from previous C-V, DLTS, and ESR measurements are plotted together on the same scale. The two P_b peaks account for about half the total integrated trap density ($Q_{it} \approx 8 \times 10^{12} \text{ cm}^{-2}$) between $E_v + 0.2\text{eV}$ and $E_v + 0.9\text{eV}$. The n-type samples had a slightly lower integrated concentration, about $5 \times 10^{12} \text{ cm}^{-2}$. It is worth mentioning that the energy resolution of interface state distributions obtained by C-V and DLTS is about 3.5kT and 2.5kT, respectively, i.e. no better than

about 0.1eV for C-V measurements at room temperature.⁽²⁴⁾ Furthermore, the entropy properties of interface traps can have a considerable influence on measured energy distributions.⁽²⁵⁾

Because of the very high interface trap concentration, there is a great stretchout of the C-V curves. Even though it is not difficult to produce accumulation or depletion conditions, as reflected by carrier capacitance at 1 MHz, it is extremely difficult to fill or empty most of the interface traps over a wide range of energy within a reasonable time interval, evidenced by the very shallow dip in the low-frequency C-V curve. Integration of the curve shows that to fill and empty traps between $E_v + 0.15\text{eV}$ and $E_v + 1.0\text{eV}$ in p-type samples requires a gate voltage range of -60 to +40V. Repeated application of such voltages would have quickly destroyed the samples, of which only a very limited number were available. In the experiments to be described here, it was therefore generally not feasible to achieve extreme trap occupancies, nor was it feasible to derive wide-range bias vs. band-bending functions at the required low temperatures. Care was taken to achieve sufficiently accumulated or depleted conditions to fulfill the needs of a meaningful measurement. Possible effects of these experimental conditions on data analysis and interpretation are presented in pertinent sections to follow.

B. Low Temperature C-V Analysis

Typical high-frequency (1 MHz) C-V curves of n-type samples are shown in Fig. 4 for different temperatures. The curves were obtained by sweeping the gate voltage from +5 to -15V and back to +5V with a rate of 100 mV/s. Two features are of particular interest: (1) the part of the curves which is due to depletion of majority carriers in the space charge region moves with decreasing temperatures to larger positive voltages; (2) for temperatures lower than about 250K a ledge appears in deep depletion, since electron emission is too slow at this particular sweep rate of 100 mV/s.⁽⁶⁾ The size (with respect to the capacitance) and the position (with respect to the gate voltage) of the ledge do not depend on the accumulation voltage in the range between 0V and +30V. This implied that at a constant temperature, the C-V curve did not change markedly above a certain accumulation voltage due to the recharge of the defect which caused the ledge, whether or not the measurement were performed in thermal equilibrium or after illumination. At 160K this was valid for any voltage above 0V. Thus, the n-type samples were usually run with accumulation voltage around +5V.

Since the hysteresis is caused by electron emission, the position and size of the ledge depend on the sweep rate of the gate voltage.⁽⁶⁾ The size and position of the

ledge are rather independent of the sweep direction, i.e. whether the voltage sweep starts at +5V going to -12.5V and back or whether it starts at -12.5V and goes to +5V and back. For convenience the C-V curves were always taken by sweeping the gate voltage from negative values to positive values and back.

If the n-type MOS device is kept in depletion (i.e. -12.5V) at sufficient high temperature after the initial accumulation, the capacitance will relax in darkness towards equilibrium because the defects are thermally emitting their charges and therefore a change in capacitance is observed. Since the capacitance of the C-V ledge increases with time and the sample in this example is n-type, this means that either electrons are emitted or holes are captured. The capacitance increase depends on the temperature and can be accelerated at low temperatures by momentary illumination with sub-half-bandgap light. This implies that electrons are emitted and not holes, i.e. that the sample is not in inversion at -12.5V. This is shown in Fig. 5, where two C-V curves are presented. Both were taken at 160K in darkness, one after about 3 min in darkness and the other after illumination with white light. The shape of the ledge after illumination did not depend on the photon energy, i.e. whether above-band-gap, sub-bandgap or sub-half-bandgap light was used, as long as the photon energy was larger than about 0.4eV and steady-state was achieved. Since steady-state was readily obtained even with sub-half-bandgap light it has to be assumed that the upper capacitance curve of the ledge in Fig. 5 corresponds to the case where most of the upper P_b levels are empty.

When the device was inversion-biased to -30V at 160K, the depletion part of the C-V curve shifted to more negative voltages. The original C-V curve could be restored by heating the sample to 230K for about 3 min. These effects did not change the size or position of the ledge. At 100K the C-V curves showed features similar to those presented by Chang et al.⁽¹²⁾ In darkness (i.e. without illumination prior to measurement) the C-V curve showed no ledge at this temperature, and no change was observed with time.

Similar considerations apply for p-type samples. Apart from the polarity no qualitative differences were observed.

C. Optical Measurements

The spectral distribution of the photoionization cross section was measured for holes in p-type samples and for electrons in n-type samples at about 60°K using the initial slope technique.⁽²³⁾ It was found that absorption in air considerably influenced the photoionization thresholds and that all spectral distributions

therefore had to be measured with a vacuum spectrometer. The bias of the sample was always chosen such that the measurements were executed in deep depletion, well within the ledge. Care was taken that for every measuring point, the level to be studied was equally occupied by majority carriers, since the observed threshold energy can be affected by inadequate filling of the level. In most measurements this was achieved by switching the sample from accumulation. It was found that the capacitance due to the large signal amplitude increased almost linearly with time at the very beginning of the transient when illuminated with monochromatic light of variable wavelength and that the change in capacitance was persistent when the light source was switched off. It has been shown previously⁽²³⁾ that the slope of the capacitance change due to an almost completely occupied level is proportional to the photoionization cross section of the excited charge carrier. If the center is only partially occupied, a different proportionality factor is needed. As long as the initial occupancy of the center is constant, the photoionization spectrum is readily measured by the initial slope technique.

The spectral distribution measured in p-type samples is shown in Fig. 6. The threshold is at 0.38 eV. At about 38 meV above threshold a subsidiary increase of the cross section is observed, suggesting that an additional excitation process is contributing to the spectral distribution. Since the spin-orbit split-off band lies about 42 meV below the valence bandgap, it seems rather probable that the extra contribution is due to the split-off band. Above about 0.6 eV, the spectral distribution is completely smooth, indicating that a possible excitation involving the second trap peak level of the p-type Si is much weaker than the excitation of the first trap peak level. The spectral distribution of e_p^0 with a rather well defined threshold energy suggests that a possible complication of the initial slope technique due to an energy distribution of the interface states is obviously not as disturbing as one might have expected.⁽²⁶⁾

All samples showed some photosensitivity for photon energies smaller than 0.38 eV. Our equipment did not allow us to measure spectral distributions accurately in this energy range because of the small signal and the low intensity of our light sources. We can therefore not decide whether the signal for these photon energies is due to stray light of higher energy or caused by carrier excitation in the sample at these particular energies. Previous studies by photocurrent transient spectroscopy on n-type and p-type MOS capacitors have shown nearly complete depopulation of P_b centers after about one hour by 0.37 eV photons of a He-Ne laser at low temperatures (i.e., ≤ 56 K).⁽²²⁾ Similar phenomena in the case of bulk traps have been ascribed to excited states. Such bound-to-bound transitions cause a capacitance change if the excited charge carriers are then thermally excited into the valence or conduction band, as the case may be.⁽²⁷⁾ In the MOS system, such excitations might also involve

the continuum states.

The spectral distribution of the photoionization cross section for electrons, σ_n^0 , is shown in Fig. 7. The curve shows two main threshold energies. One is at about 0.35eV and the second one at about 0.8eV. As in the case of the hole spectra, there is some optical excitation below the first main threshold, presumably with analogous origins.

The second threshold at about 0.8eV was carefully substantiated, and represents excitation of electrons into the conduction band, as seen from the increase of the capacitance due to illumination. This threshold can be explained by two different excitation processes if it is assumed that some of the P_b centers remain singly occupied during application of the accumulation bias: (1) photoexcitation of electrons from the lower trap level into the conduction band and (2) photoemission of holes from singly occupied centers and subsequent photoexcitation of the electrons from the doubly occupied center.⁽¹⁵⁾ The symmetrical position of P_b levels in the gap precludes distinction between the two possibilities on an energy basis. Whichever explanation is correct, however, it is of interest that a similar higher energy transition is not observed in p-type Si, since the ionization curve is otherwise very similar to n-type. A comparison of the absolute cross section values presented in Figs. 6 and 7, however, suggests that the second threshold probably is caused by photoexcitation of electrons from the lower trap level.

Exponential optical decays were obtained at low temperature when instead of the depletion bias the photo capacitance was kept constant. The insert of Fig. 6 shows an example of an p-type sample which was obtained for 0.565 eV light causing an increase of the depletion bias with an exponential transient over more than one order of magnitude. Since the number of photons striking the sample in this example was about $3.8 \cdot 10^{16} \text{ cm}^{-2} \text{ s}^{-1}$, a value of $3.6 \cdot 10^{-19} \text{ cm}^2$ is obtained for the photoionization cross section of holes at 0.565 eV.

D. Electrical Measurements

Thermal emission and capture were measured in both n- and p-type samples by single-shot techniques.⁽⁵⁾ Thermal emission of holes from the lower bandgap level in p-type samples was investigated by first heating the device to 230K with -5V accumulation bias and then cooling the sample to the temperature at which the thermal emission rate was measured. When the capacitance had stabilized, showing that the sample had reached the desired temperature, the device was zero biased, resulting in a fast decrease of the capacitance followed by a much slower exponential

increase. A typical transient obtained for 184K is shown in Fig. 8. In the insert the increasing capacitance signal is plotted semilogarithmically, showing that the transient is a single exponential over at least two orders of magnitude. From the slope of the semilogarithmic plot the absolute value of the hole emission rate is readily calculated for this particular temperature, giving $e_p^t(184.3K) = 6.10^{-2} \text{ s}^{-1}$. The positive capacitance transient proves that the signal is due to hole emission, not electron emission. As mentioned earlier at these temperatures and voltages we have good reasons to believe that no inversion layers are formed and that an increase in capacitance due to thermal generation of minority carriers can therefore be excluded. An Arrhenius plot of hole emission rates e_p^t obtained at different temperatures is presented in Fig. 9, giving an activation energy of 0.35 eV. This energy is unspecified; but, since e_p^t/T^2 is plotted versus $10^3/T$, it is equal to the enthalpy if the hole capture is temperature independent. To complete the analysis, it is necessary to know the temperature dependence of the capture process.

It should be noted that the accumulation bias (-5V) is probably not sufficient to empty all centers completely, as explained earlier. However, the bias was chosen to empty the lower level adequately; and further, great care was taken to assure the same initial occupancy throughout the experimental run. As seen from Fig. 4 and 5 this was easily achieved since the size and position of the ledge was not dependent on the accumulation bias. Some further aspects of this procedure are discussed later.

Thermal emission of electrons from the doubly occupied level in the upper half of the bandgap in p-type samples was likewise done by single shot measurement. The sample was put into deep depletion (+5V) at about 230K and then cooled to 189K. The sample was then zero biased, resulting in a fast capacitance increase due to the voltage change, followed by a slower capacitance decrease, Fig. 10. The decrease suggests that the signal is due to thermal emission of electrons and not holes, since in the latter case a capacitance increase would be expected. Plotting the decrease of capacitance semilogarithmically (as shown in the insert of Fig. 10) gave a single exponential over two orders of magnitude. From the slope of this plot, the thermal emission rate of electrons e_n^t for the upper level was calculated. Performing these measurements at different temperatures and plotting the electron emission rate e_n^t/T^2 versus $1/T$ resulted in a straight line with an activation energy of 0.31eV, Fig. 9.

Measurements of thermal electron emission from the upper level were also executed with n-type samples. Instead of heating to 230K as in the case of p-type samples, the n-type samples were first warmed to 180K under accumulation bias (+10V), and then cooled to the temperature at which the study was performed. When the temperature had stabilized the diode was zero-biased, and the time

dependence of the capacitance increase recorded. All transients appeared singly exponential over more than an order of magnitude. Performing these measurements at different temperatures and plotting the electron emission rates e_n^t/T^2 in an Arrhenius plot (Fig.11) resulted in a straight line with an activation energy of 0.29 eV, in good agreement with similar results on p-type samples.

Investigation of the hole emission from the lower level in n-type material were performed in a manner similar to the electron emission in p-type material by cooling the samples from 180°K under depletion bias (-30V). After zero biasing the sample, a fast capacitance increase was observed, followed by a much slower capacitance decrease. The transients due to the capacitance decrease were singly exponential over more than an order of magnitude at all temperatures studied (120-150°K). From an Arrhenius plot of e_p^t/T^2 an activation energy of about 0.29eV was derived from the hole emission in n-type material, in fair agreement with the p-type result and DLTS measurements.

The thermal emission of holes for the lower level and of electrons for the upper level was also studied in p-type samples by using conventional DLTS. In both cases well resolved DLTS peaks were observed, as in Fig. 12a for hole emission. An Arrhenius plot of the hole emission rates e_p^t/T^2 reveals an activation energy of 0.31 eV (Fig.12b), somewhat smaller than the one obtained from single shot measurements in p-type samples but in good agreement with the single shot measurements in n-type samples. For a continuous distribution of interface states one would expect a rather featureless DLTS spectrum with a smoothly-varying signal over the entire temperature range⁽²⁸⁾. The fact that we obtained very similar activation energies from DLTS and single shot measurements in both n- and p-type material with very different initial conditions suggests that we probably rather deal with a peak in level distribution than with a distribution in occupancy. Similar studies of the electron emission in p-type samples showed two emission peaks with activation energies of 0.31eV and 0.37eV. The peaks seen for e_p^t were positive, whereas in the case of e_n^t only negative peaks were observed. Since conventional DLTS measurements on MOS capacitors can detect only majority-carrier emission and surface generation through interface states for depletion-bias conditions⁽²⁸⁾, it has to be assumed that the negative peaks arise from minority-carrier recombination. These measurements were performed on two different samples, both giving essentially the same results.

The thermal emission of electrons was similarly studied in n-type samples by DLTS. Well resolved peaks were observed for all windows used. An Arrhenius plot of the thermal emission rates e_n^t/T^2 obtained in this way gave an activation energy of 0.35eV, in reasonable agreement with the single shot measurements.

Hole capture in p-type samples was studied using the pulse train method.⁽⁵⁾ The sample was put into depletion and illuminated with sub-bandgap light prior to the measurement, to make sure that lower levels were filled with electrons. After removing the light source the sample was accumulation-biased by a 18 μ s pulse, resulting in a small, persistent decrease of the capacitance. The decrease of the capacitance proves that holes and not electrons are captured. Plotting the capacitance semilogarithmically as a function of the number of pulses applied, a single exponential straight line was obtained. Typical data obtained at 110K are shown in Fig. 13. From these measurements the absolute value of the hole capture cross section is easily calculated⁽⁵⁾ if the number of free holes, present during the capture process, is known. The measurement of free carriers at the interface of an MOS structure is not straightforward; in fact, the surface concentration of free carriers decreases with time as interface states are filled during the accumulation pulse.⁽²⁸⁾ No attempt was made to perform a rigorous determination. Assuming a value of $10^{15} - 10^{16} \text{ cm}^{-3}$ for the free carrier concentration gives a value of about $10^{-18} - 10^{-19} \text{ cm}^2$ for the hole capture cross section. These measurements were performed at different temperatures in the range between 87K and 125K. The measured values varied by about $\pm 25\%$ without showing any temperature trend, Fig. 14. These results are in good agreement with previous measurements, using the energy-resolved DLTS technique on similarly-processed MOS capacitors which likewise established that the capture cross section for the characteristic interface states is essentially constant.^(28,30) In our further discussion it is therefore assumed that the hole capture cross section is not significantly dependent on temperature and that the activation energy obtained from the different Arrhenius plots of e_p^t/T^2 is an enthalpy ΔH_p . Investigations performed with two different p-type samples resulted in the same enthalpies, but gave slightly different values for the hole emission rate.

Since the cryostat which was available for our measurements only allowed for temperatures down to about 85K and the thermal emission of electrons is observed at lower temperatures than in the case of holes, the electron capture into the upper level could only be studied qualitatively. These measurements suggested that the electron capture obviously is not very dependent on temperature. It is therefore assumed that, as in the case of holes, the capture cross section of electrons is temperature independent and that the activation energy in the electron emission measurements is close to the enthalpy.

E. Hydrogen Annealing

The G-V analysis reflects the dominance of interface traps over bulk traps in the samples studied. However, the very high sensitivity of the electrical and optical

techniques used makes it desirable to further delimit the possible contributing trap species. In spite of several attempts it was not possible to produce sufficient optical modulation of the ESR signal to correlate directly with the photocapacitance and electrical analysis. This may be due to the low optical cross section of P_b centers. Indirect means were therefore necessary. Hydrogen is known to anneal both interface traps and P_b centers; in fact, the two show quantitatively identical annealing kinetics, with $T_a \approx 220^\circ\text{C}$.⁽³¹⁾ After many of the measurements were completed, one of the samples was annealed for 20 minutes in forming gas at 400°C . The ESR signal (Fig. 15), the stretchout in the C-V curve, and the trap ledge in the C-V curves were all eliminated. In particular, the sample became almost completely insensitive to light even at 180°K . After about 10 days, the electrical manifestation recovered somewhat; but electrical signals remained an order of magnitude weaker than the unannealed values. Interestingly, physical parameters derived from electrical or optical measurements did not change, despite the far fewer traps present.

IV. Analysis and Discussion

The photon energies and general character of the principal optical photoionization responses at about 0.4eV are very well correlated with the two peaks in the interface trap spectrum from C-V or ESR. The $\sim 0.1\text{eV}$ difference between the optical hole threshold at about 0.4eV (Fig. 6) and the lower trap level at 0.3eV (as observed by C-V or ESR) may be interpreted as a configurational change in the trapping center with electron occupancy. This has been calculated for P_b by a molecular orbital approach to be about 0.1eV;⁽³²⁾ the experiment and the theory are consistent. A similar but smaller difference for the electrical/ESR (0.3eV) and optical (0.35eV) energy for the upper level (Fig. 7) presumably indicates the same effect, though theoretical calculation is more complicated for this case and has not been attempted. The occurrence of a second major threshold at about 0.8eV in the case of electron excitation in n-type samples (Fig. 7) is assigned to ionization of the single electron remaining in the amphoteric⁽¹²⁾ trap after the first ionization. The position of the lower level via this ionization route is about 0.4eV above the valence band. For small lattice relaxations the level positions, and associated optical cross-sections, are in reasonable accord with theory.⁽³³⁾ Because of the generally good correlation of photoionization features with established properties of the P_b center, and because of the dominance of P_b over other traps in the samples, it seems very reasonable to assign the photocapacitance results to P_b centers.

The activation energies for thermal carrier emission correlate closely with the P_b energy level positions observed by equilibrium techniques at room temperature, viz., C-V and gated ESR. For the transition between valence band and the lower

level of the interface trap distribution, the single-shot thermal energies in this study average 0.32eV; previous C-V measurements yielded 0.26eV and ESR, 0.30eV. For the transition between the upper trap level and the conduction band, our single-shot thermal energies average 0.33eV while previous C-V measurements gave 0.28eV, and ESR, 0.32eV. Considering that the ESR studies were performed at room temperature whereas the electrical measurements described in this paper were executed at low temperatures, good agreement is obtained between our thermal data and previous ESR results.

Nonetheless, there is a puzzling aspect to the emission results. Two interesting features of the observations are the steep onset of photoionization and the single-exponential character of the capacitance transients observed in various electrical and optical experiments. Single-exponential capacitance transients were only observed for measurements performed within the ledge of the C-V curve shown in fig. 5. These phenomena both suggest trap levels narrower than those seen as peaks in gated ESR and ESR hyperfine linewidth, which indicate P_b center level distribution width for ~ 100 meV. This discrepancy may indicate that the trap levels are narrower than previously assumed or that the discrepancy is only seeming and can be at least partially explained by experimental factors. Since thermal measurements inherently are caused by collective excitation processes they give little direct information on the energy distribution of energy states. The circumstances are somewhat better for optical excitation processes.

In addition to the experimental factors, the physical nature of the trap system may play a part. The role and behaviour of the continuum traps were not separately studied; they may act in series or parallel with P_b centers with uncertain effects on the observed behavior. Another possible factor is the usual randomly-distributed oxide fixed charge, providing local electric fields which would broaden D_{it} peaks observed in gated electrical or EPR methods, but would not necessarily affect photoionization. For all these reasons, the electrically-observed parameters, studied previously or in this paper, are not exclusively assigned to P_b centers, although the P_b centers appear to play a major role.

The hydrogen annealing has another meaning beyond the excellent correlation of signal strengths from ESR and electrical measurements. Silicon dangling-orbital centers are the only well-defined defects in Si which anneal in H_2 at 400°C and below; all the other common bulk traps require 700°C or higher temperatures.^(7,34) This further reduces the likelihood of interference in our observations from the familiar bulk trapping impurities. In addition, the presence of bulk Si-dangling-orbital defects (as opposed to interface P_b centers) is ruled out by absence of the characteristic bulk D-center ESR signal, readily differentiated from the

P_b signal. Thus on several counts, it is likely that P_b centers dominate many of the effects presented here. Nonetheless, possible contributions from undefined weak-bond states in the U-shaped continuum (which are also H_2 -annealable at low temperature) cannot be ruled out.

V. Concluding Remarks

An important conclusion for this entire investigation is the overall great similarity of behavior of MOS interface traps to the numerous bulk Si traps which have been studied by junction space charge methods.^(4,5) The general character of phot capacitance, single-shot, pulse train, and DLTS results is much like that observed for many other deep levels in silicon and other semiconductors.

Photocapacitance experiments on interface traps show sharp ionization thresholds at energies 0.05-0.1eV different from those determined for the two levels of the P_b center by dark capacitance, C-V and gated ESR. Since in the latter cases the system is in its relaxed state throughout the observations, the displacement of the optical threshold seems very likely to be the Franck-Condon shift associated with a configurational change in the center with different electron occupancy. Thus on the basis of the overall consistency of the picture, the photoionization results are ascribed to the P_b center, which is clearly the dominant trap present. Furthermore, absolute values for the photo ionization cross section of electrons and holes of the P_b center are presented for the first time.

Electrical measurements presented here also show aspects which are consistent with assignment to P_b centers, such as the clear emergence of discrete levels and the energies of activation for thermal hole and electron emission. It should be noted that the sign of the dark capacitance transients was consistently in agreement with what one would expect from the various initial conditions and that the enthalpies for the upper and lower level are very similar irrespective whether they were measured in n-type or p-type samples. However, there is a discrepancy in the observed exponential electrical transients compared with previous findings. Exponential transients would otherwise imply a narrow width for the pertinent trap energy level. It is not clear whether they arise from experimental conditions used or from undemonstrated features of MOS interface traps, such as the participation of band-tail states. Thus we do not make definite assignments of the single-shot emission energies and rates to P_b centers at this time.

Direct optically-stimulated ESR would greatly assist the interpretation of effects described here. The apparent reason for the difficulty of this experiment is the

low optical cross-section of P_b centers, typically in the 10^{-20} to 10^{-17} cm^{-2} range for the various trap-filling or emptying transitions with the exception of e_n^0 for the lower level.⁽³³⁾ This compares to 10^{-16} to 10^{-15} cm^{-2} for many other impurities in bulk silicon, for example.⁽²⁷⁾ The photocapacitance technique is so much more sensitive than ESR that it is not greatly burdened by the low cross-sections. Photo-ESR experiments would enable much firmer assignments; and, hopefully, serve to isolate possible contributions by the continuous states.

Acknowledgements

The experimental work described in this paper was initiated and largely performed at Fort Monmouth. Two of us (HGG and DJK) wish to thank the Electronics Technology and Devices Laboratory for hospitality extended to us during the period September-December 1987. We thank A. H. Edwards, S. A. Lyon, E. H. Nicollian, and M. Schulz for helpful discussions and other assistance. Work at Xerox Palo Alto Research Center was supported by the U.S. Army Laboratory Command. The optical measurements performed by L. Montelius are gratefully acknowledged.

References

1. E. H. Poindexter and P. J. Caplan, J. Vac. Sci. Technol. XXX, XXX (1988)
2. N. M. Johnson and E. H. Poindexter, EMIS Datareviews Series XXX, XXX (1988)
3. G. J. Gerardi, E. H. Poindexter, P. J. Caplan, and N. M. Johnson, Appl. Phys. Lett. 49, 348 (1986)
4. See for example: C.T.Sah, L.Forbes, L.L.Rosier and A.F.Tasch, Solid-State Electron. 14, 41 (1971)
5. H. G. Grimmeiss and C. Ovrén, J. Phys. E: Sci. Instrum. 14, 1032 (1981)
6. E. H. Nicollian and J. R. Brews, MOS (Metal-Oxide-Semiconductor), Physics and Technology (Wiley-Interscience, New York, 1982), pp. 45 and 362
7. W. Fahrner and A. Goetzberger, Appl. Phys. Lett. 21, 329 (1972)
8. M. Schulz, Surface Science 132, 422 (1983)
9. N. M. Johnson, D. K. Biegelsen, M. D. Moyer, S. T. Chang, E. H. Poindexter, and P. J. Caplan, Appl. Phys. Lett. 43, 563 (1983)
10. E. H. Poindexter, G. J. Gerardi, M.-E. Rueckel, P. J. Caplan, N. M. Johnson, and D. K. Biegelsen, J. Appl. Phys. 56, 2844 (1984)
11. P. M. Lenahan and P. V. Dressendorfer, Appl. Phys. Lett. 44, 96 (1984)
12. S. T. Chang, J. K. Wu and S. A. Lyon, Appl. Phys. Lett. 48, 662 (1986)
13. E. F. da Silva, Y. Nishioka, and T. P. Ma, Appl. Phys. Lett. 51, 270 (1987)
14. R. F. Pierret and B. B. Roesner, Solid-State Electronics 19, 593 (1976)
15. D. W. Greve and W. E. Dahlke, Inst. Phys. Conf. Ser. No. 50, 107 (1980)
16. K. Blumenstock and M. Schulz, in Insulating Films on Semiconductors, ed. by M. Schulz and G. Pensl (Springer-Verlag, Berlin, 1981) p. 48

17. N. M. Johnson, W. B. Jackson, and M. D. Moyer, Phys. Rev. B, 31, 1194 (1985)
18. W. B. Jackson and N. M. Johnson, Mat. Res. Soc. Symp. Proc. 46, 545 (1985)
19. C. H. Seager, P. M. Lenahan, K. L. Brower, and R. E. Mikawa, Mat. Res. Soc. Symp. Proc. 46, 539 (1985)
20. B. Henderson, Appl. Phys. Lett. 44, 228 (1984)
21. K. M. Lee, L. C. Kimerling, B. G. Bagley, and W. E. Quinn, Solid State Commun. 57, 615 (1986)
22. N. M. Johnson, Physical Evaluation of Defects in Thermal Oxides on Silicon, (US Army Laboratory Command, Fort Monmouth, NJ, 1986), p. 6
23. See for example H. G. Grimmeiss, J. Cryst. Growth 59, 40 (1982)
24. O. Engström and A. Alm, J. Appl. Phys. 54, 5240 (1983)
25. O. Engström, Appl. Phys. Lett. (1988)
26. N. M. Johnson and D. K. Biegelsen, Phys. Rev. B 31, 4066 (1985)
27. H. G. Grimmeiss and B. Skarstam, Phys. Rev. B, 23, 1947 (1981)
28. N. M. Johnson, J. Vac. Sci. Technol. 21, 303 (1982)
29. N. M. Johnson, D. J. Bartelink, and J. P. McVittie, J. Vac. Sci. Technol. 16, 1407 (1979)
30. N. M. Johnson, Appl. Phys. Lett. 34, 802 (1979)
31. E. H. Poindexter, P. J. Caplan, N. M. Johnson, D. K. Biegelsen, M. D. Moyer, and S. T. Chang, in Insulating Films on Semiconductors, ed. by J. F. Verweij and D. R. Wolters (North-Holland, Amsterdam, 1983) p. 24
32. A. H. Edwards, Proc 13th International Conference on Defects in Semiconductors, ed. by L. C. Kimerling and J. M. Parsey, Jr. (The Metallurgical Society, Warrendale, PA, 1985) p. 491

33. A. H. Edwards and W. B. Fowler, Mat. Res. Soc. Symp. Proc. 46, 533 (1985)
34. M. Schulz, Appl. Phys. 4, 91 (1974)

List of figures

1. Typical silicon MOS test chip used for electrical, optical and ESR measurements. Dimensions are in cm.
2. Wide-range C-V and G-V curves for p-type (111) Si chip. C-V trace was taken at 10 Hz, lower C-V trace at 1 MHz; G-V trace at 10 Hz; room temperature.
3. Bandgap density of interface trap levels in p-type Si, determined by electrical (D_{it}) and ESR (P_b) methods.
4. High frequency (1.0 MHz) C-V curves for n-type chip at various low temperatures.
5. Light-enhanced relaxation of capacitance (—) toward equilibrium value by emptying of interface trap levels in n-type sample previously subjected to accumulation bias; temperature 160K. C-V curve in darknes without previous illumination (- - -).
6. Spectrum of photoionization cross sections of interface traps in p-type Si; temperature 86K. The insert shows the optically-initiated transient depletion bias increase at constant photocapacitance.
7. Photoionization cross section spectrum of interface traps in n-type Si; temperature 86K.
8. Single-shot transient capacitance increase; p-type Si. First accumulated at -5V, 230K; then cooled to 184K; then zero biased.
9. Arrhenius plot of thermal emission rates of holes (O) and electrons (O) from interface traps in p-type Si, derived from several tests like those in Figs. 8 and 10, over a range of temperature.
10. Single-shot transient capacitance decrease, p-type Si. First depleted at +5V, 230K, then cooled to 189K, then zero biased.
11. Arrhenius plot of emission rates of electrons from interface traps in n-type Si.
12. (a) DLTS observation of thermal hole emission from interface traps in p-Si.
(b) Arrhenius plot of e_p^t/T^2

13. Hole capture by interface traps in p-type Si at 110K. Sample was initially depletion-biased and illuminated with white light to fill all traps with electrons, then returned to the dark, and repeatedly subjected to 18 μ s accumulation-bias pulses. The plot shows a steady exponential decrease in capacitance.
14. Temperature dependence of hole capture in p-type Si, derived from several tests as in Fig. 13.
15. ESR signal from P_b centers in p-type Si before and after anneal in forming gas (10% H_2 /90% N_2) for 20 min at 400°C.

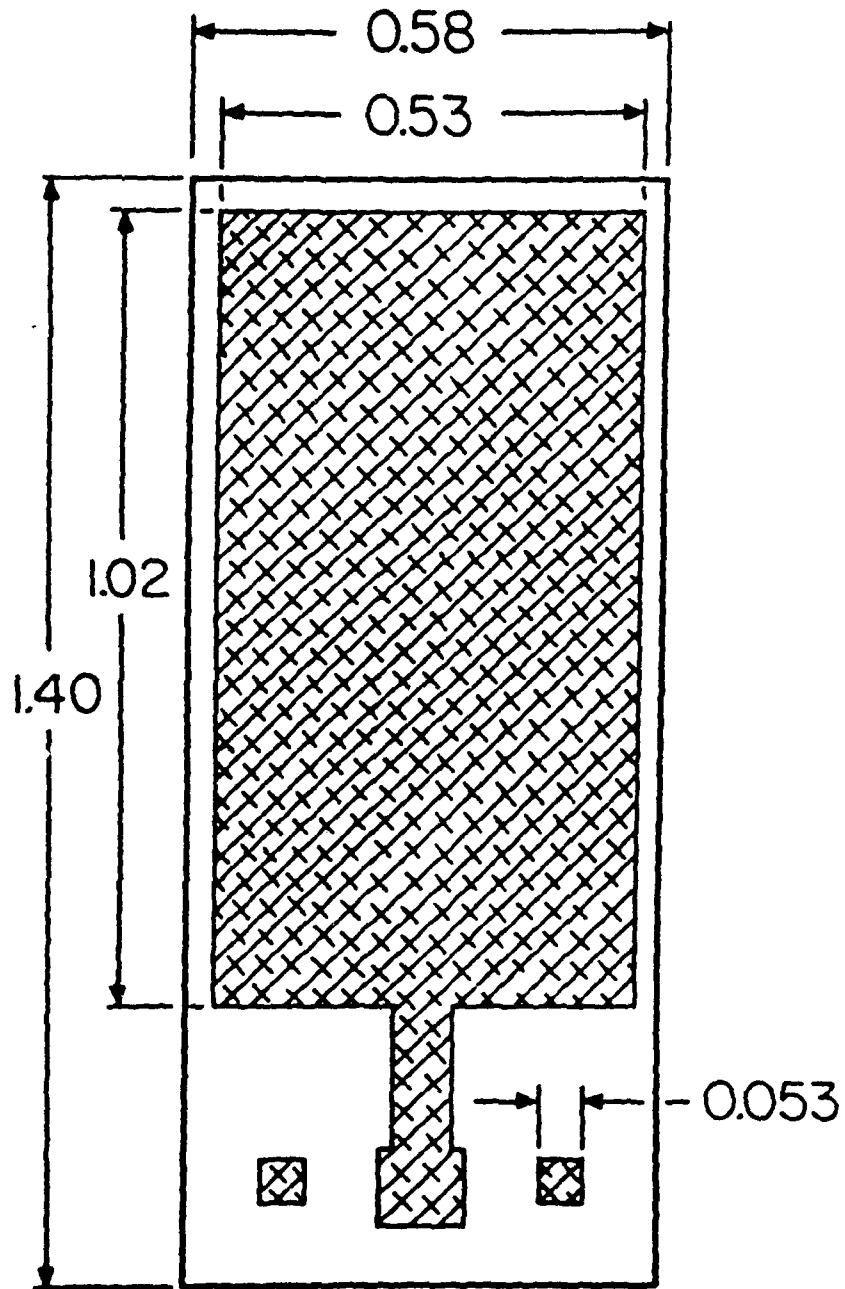


Fig. 1

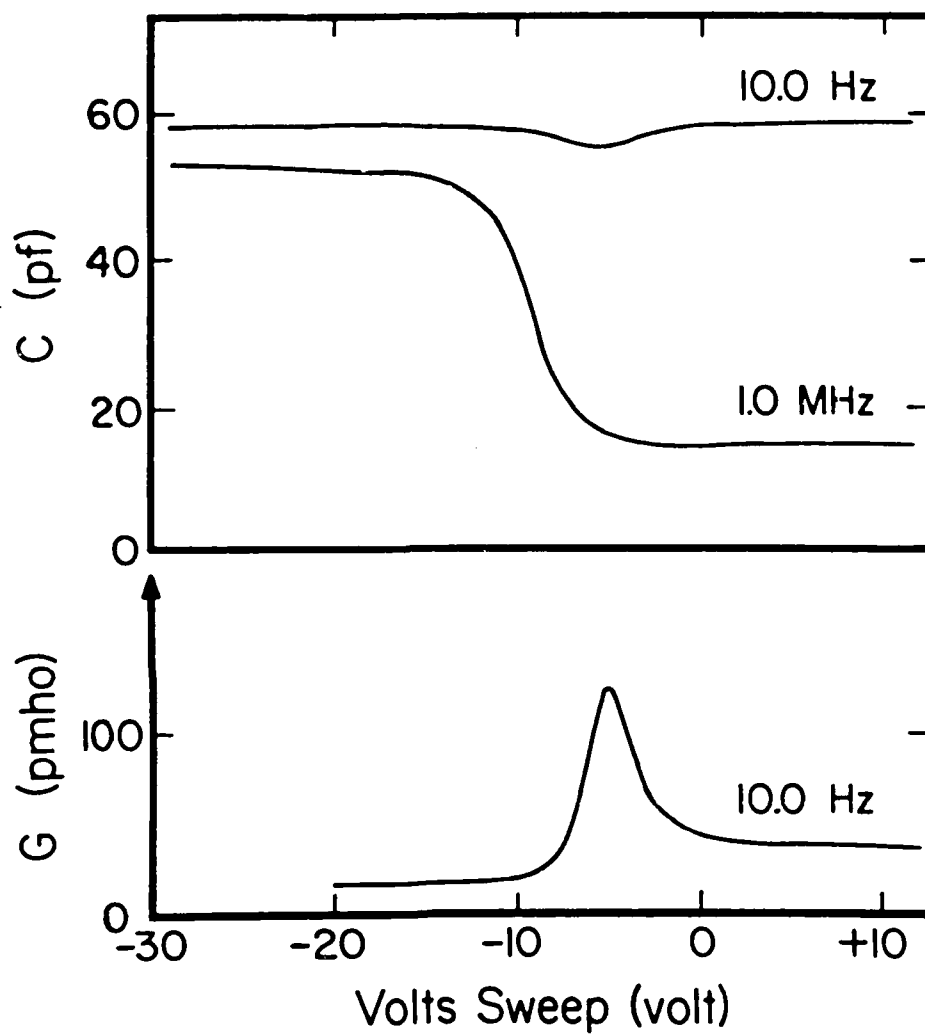


Fig. 2

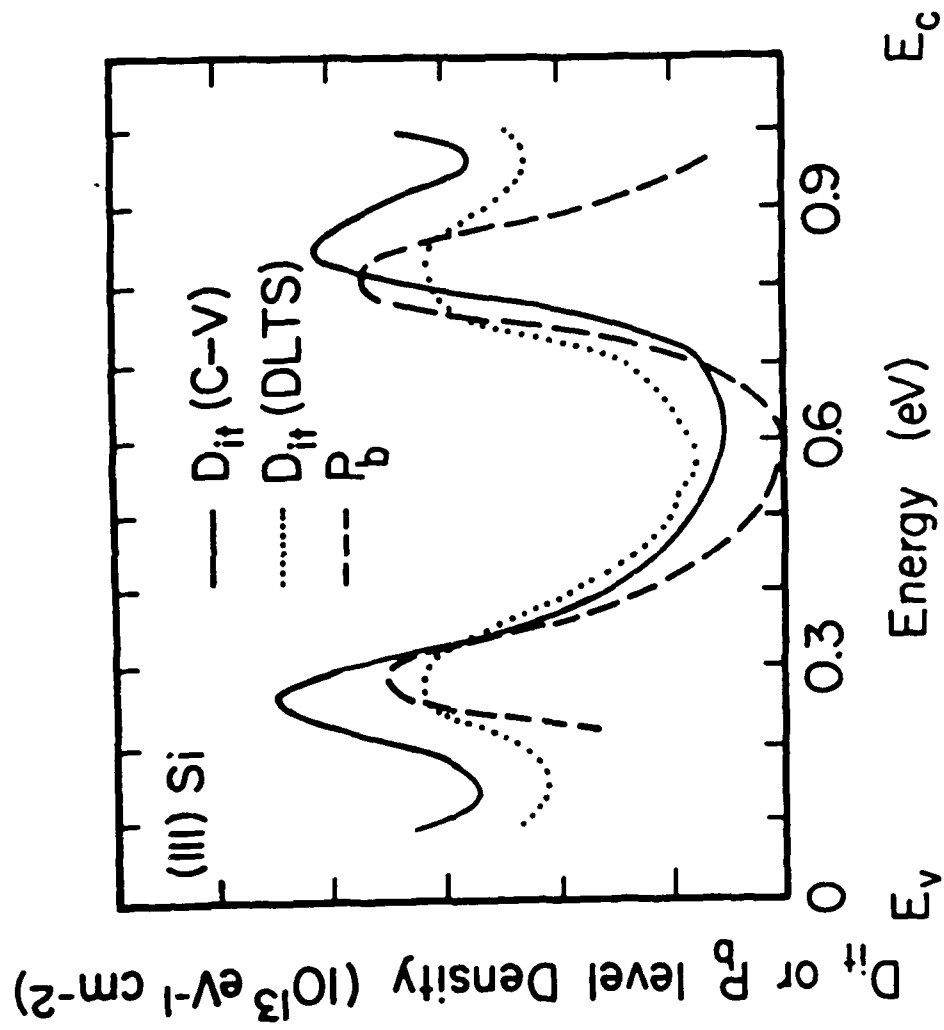


Fig. 3

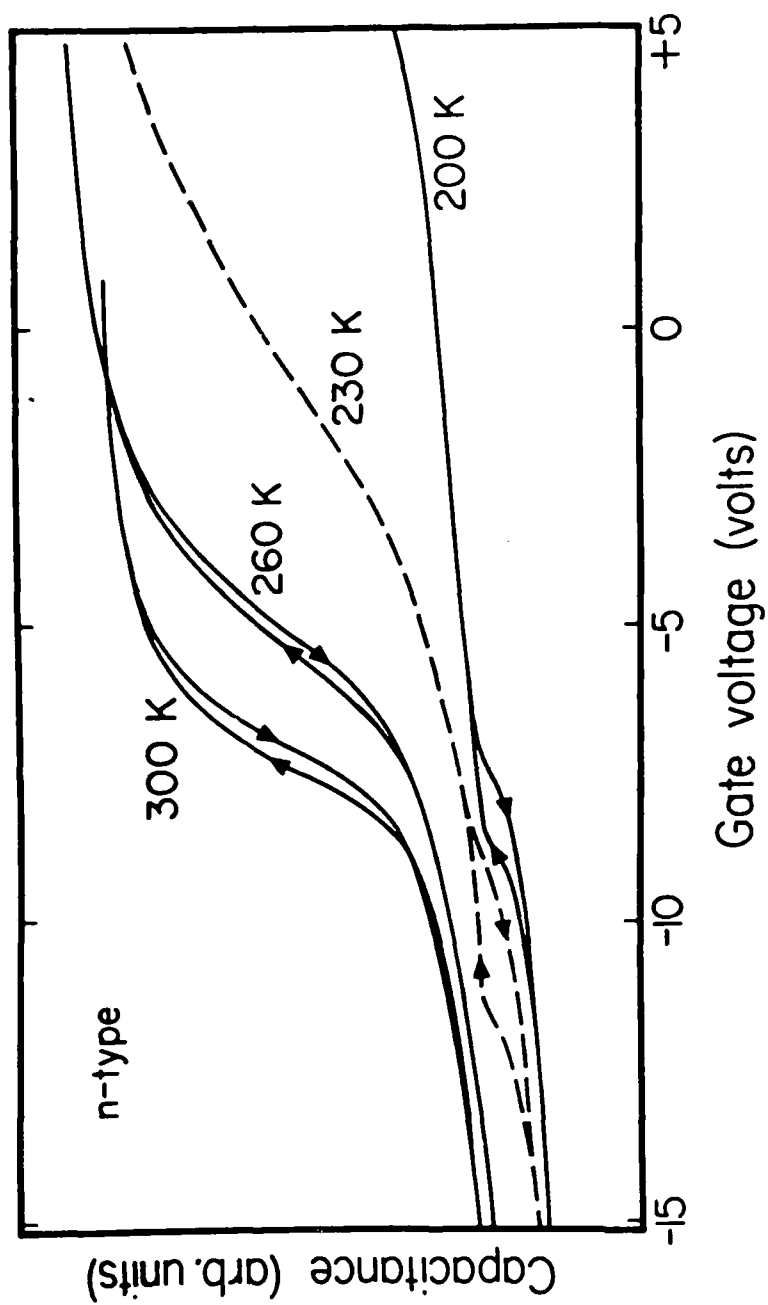


Fig. 4

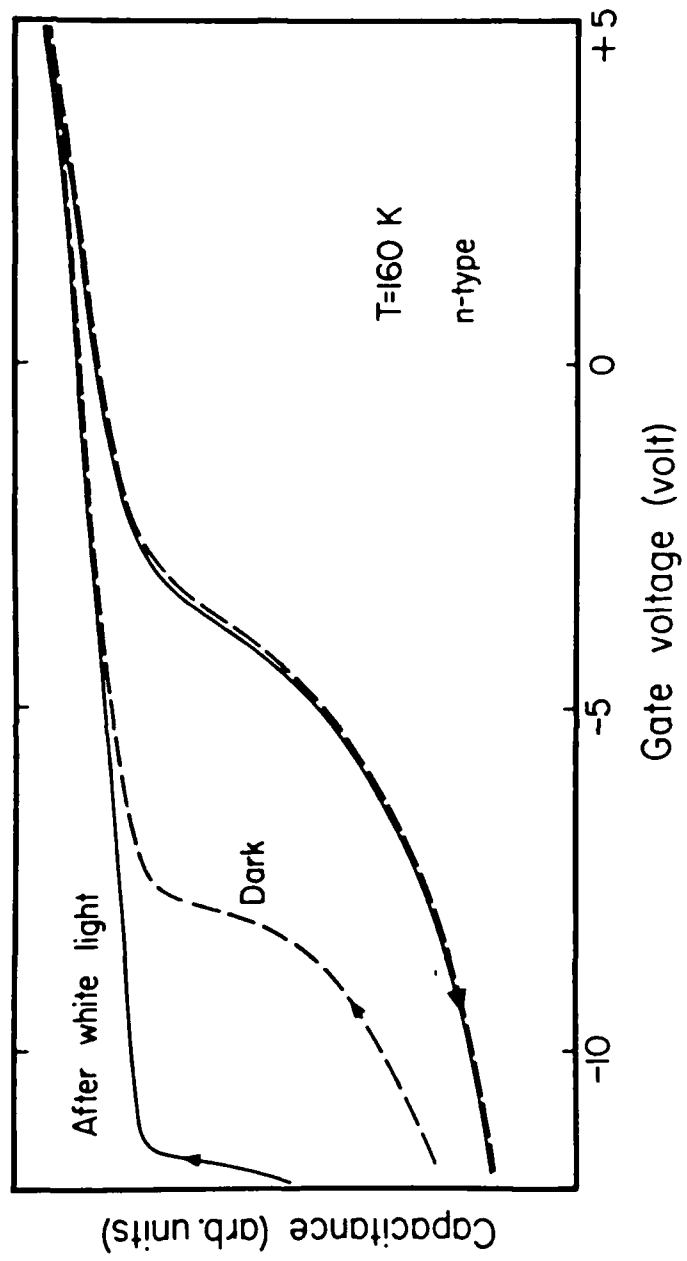


Fig. 5

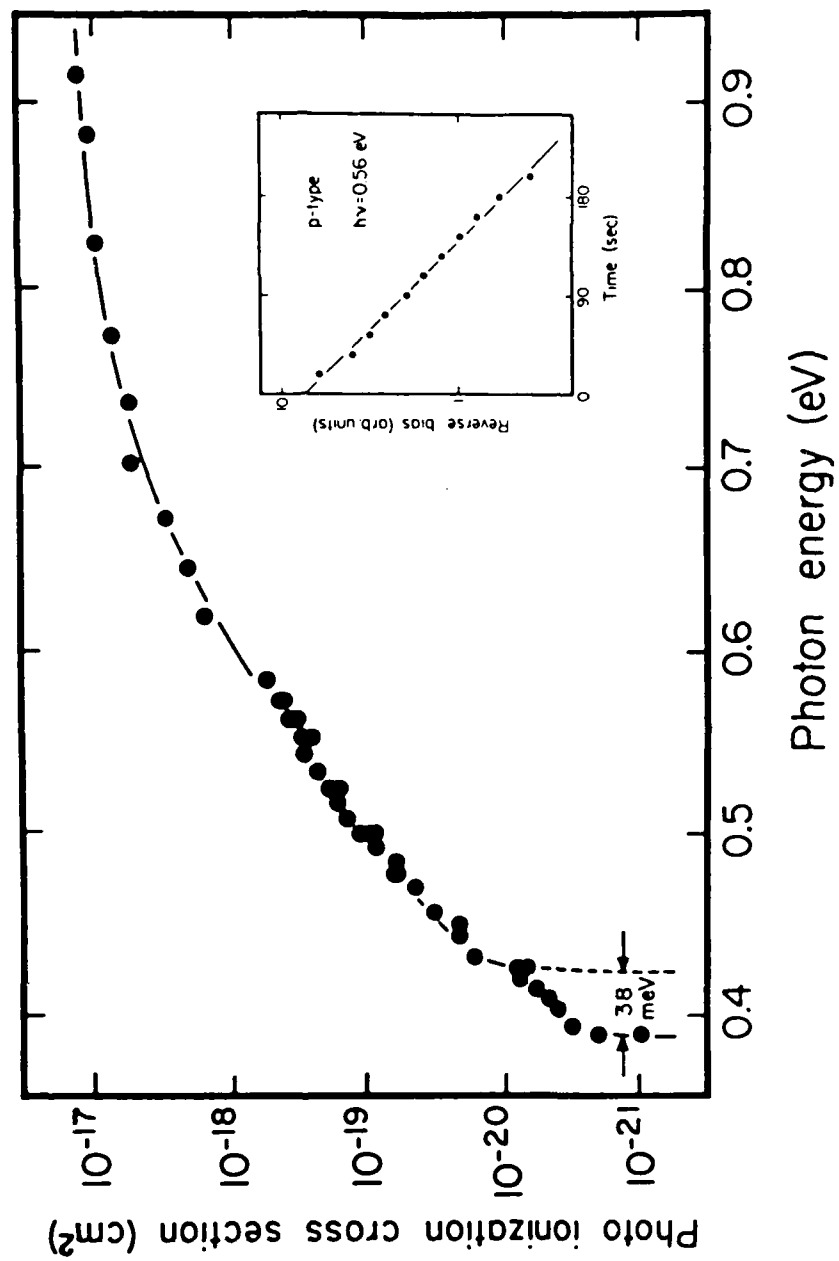


Fig. 6

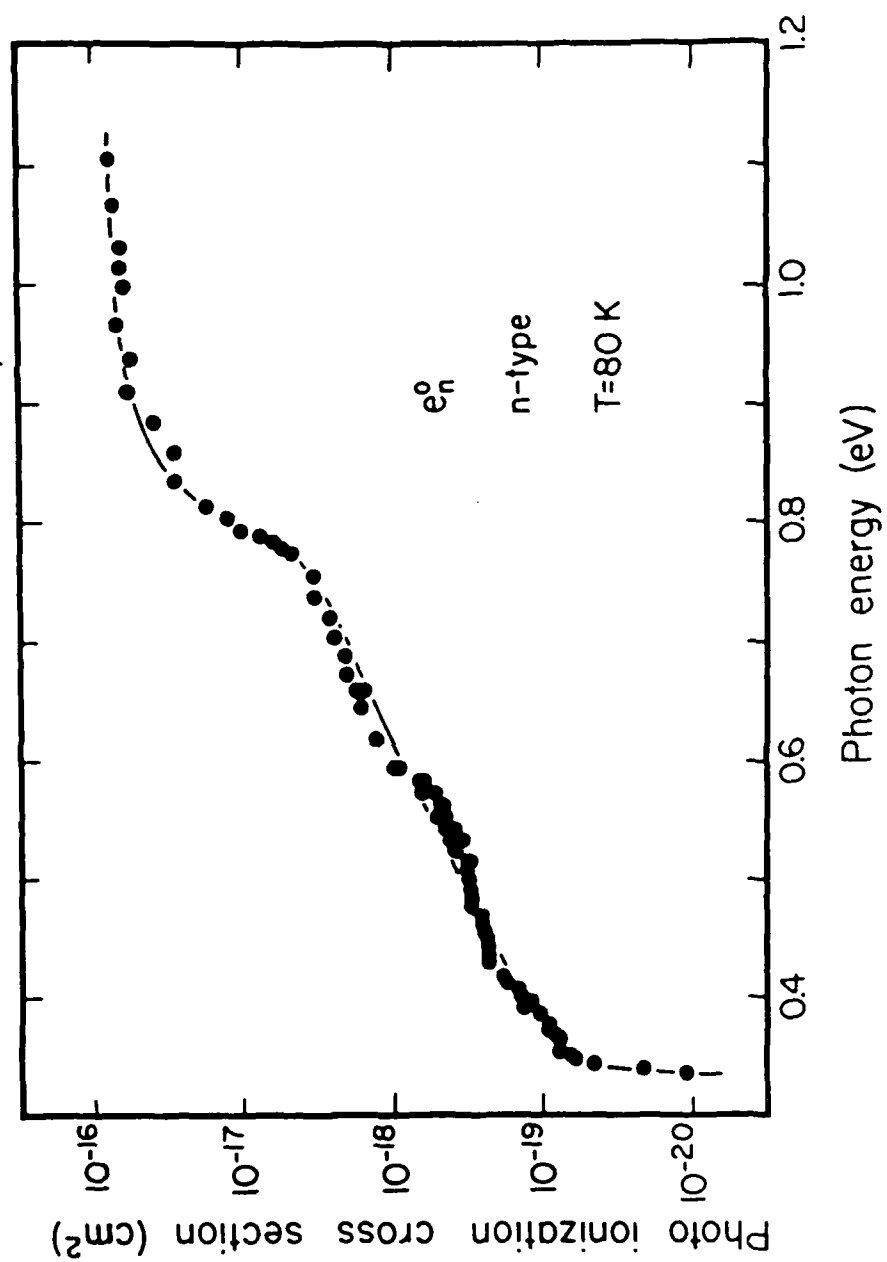


Fig. 7

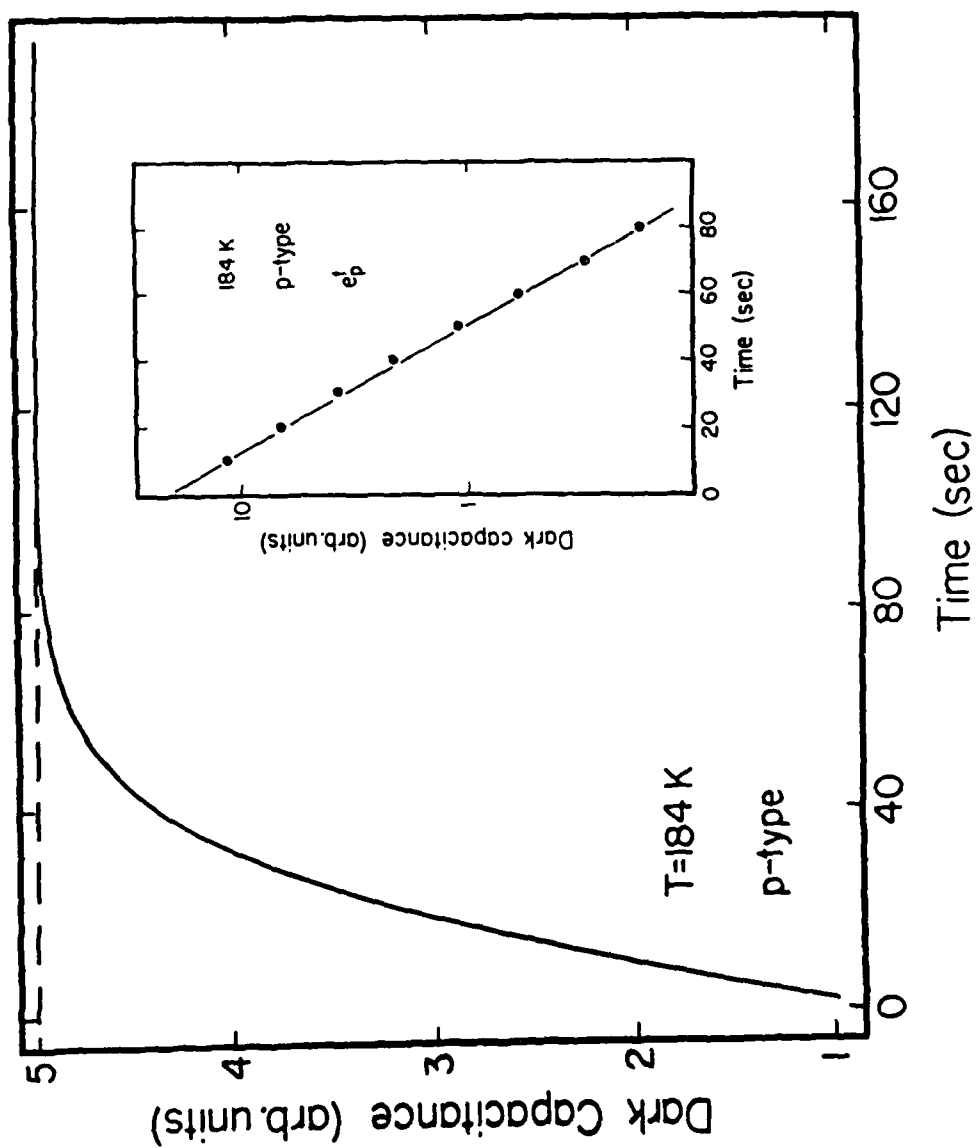


Fig. 8

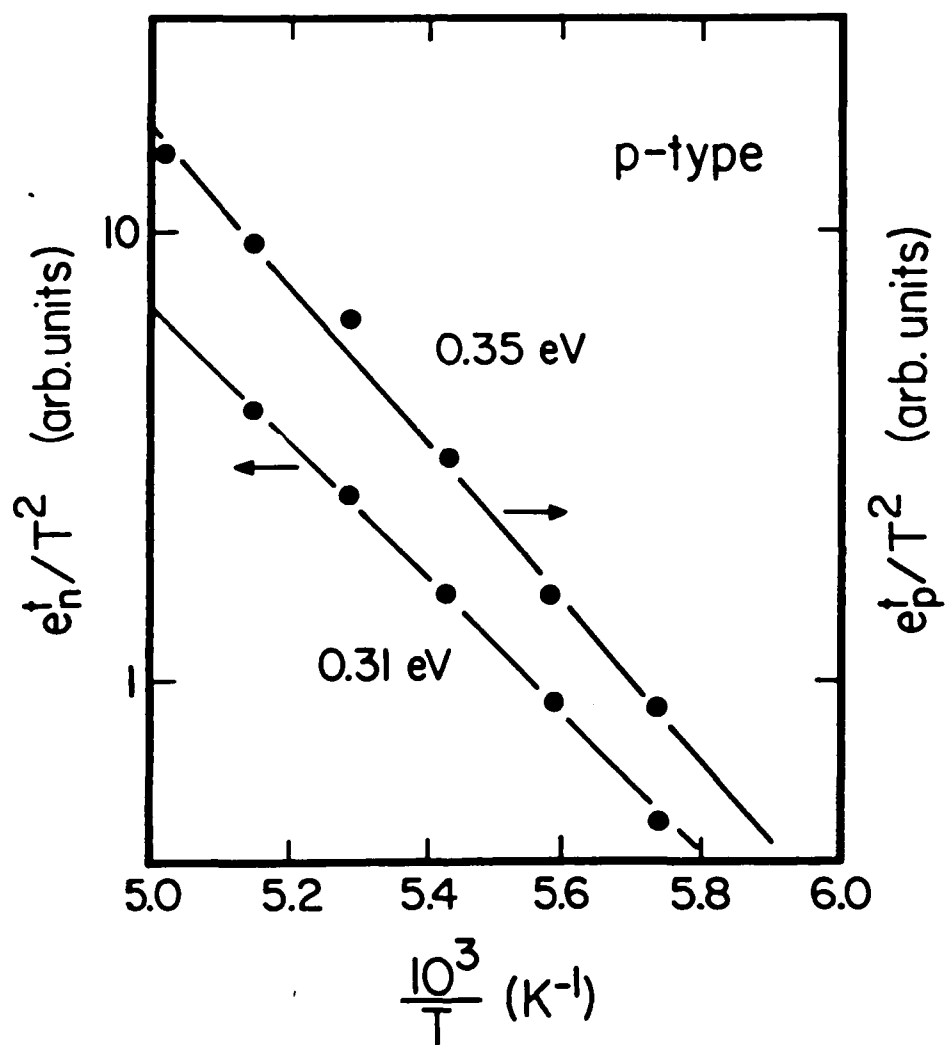


Fig. 9

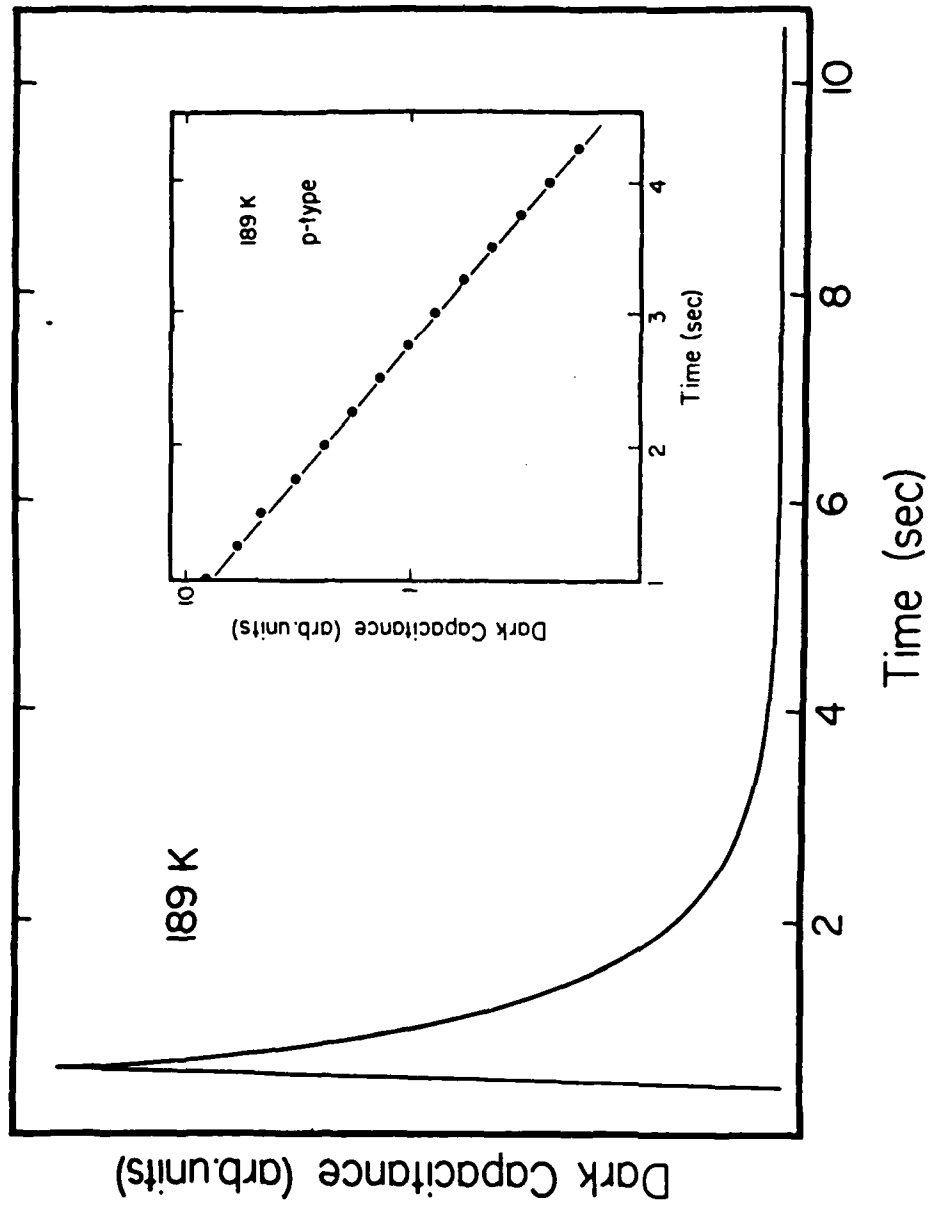


Fig. 10

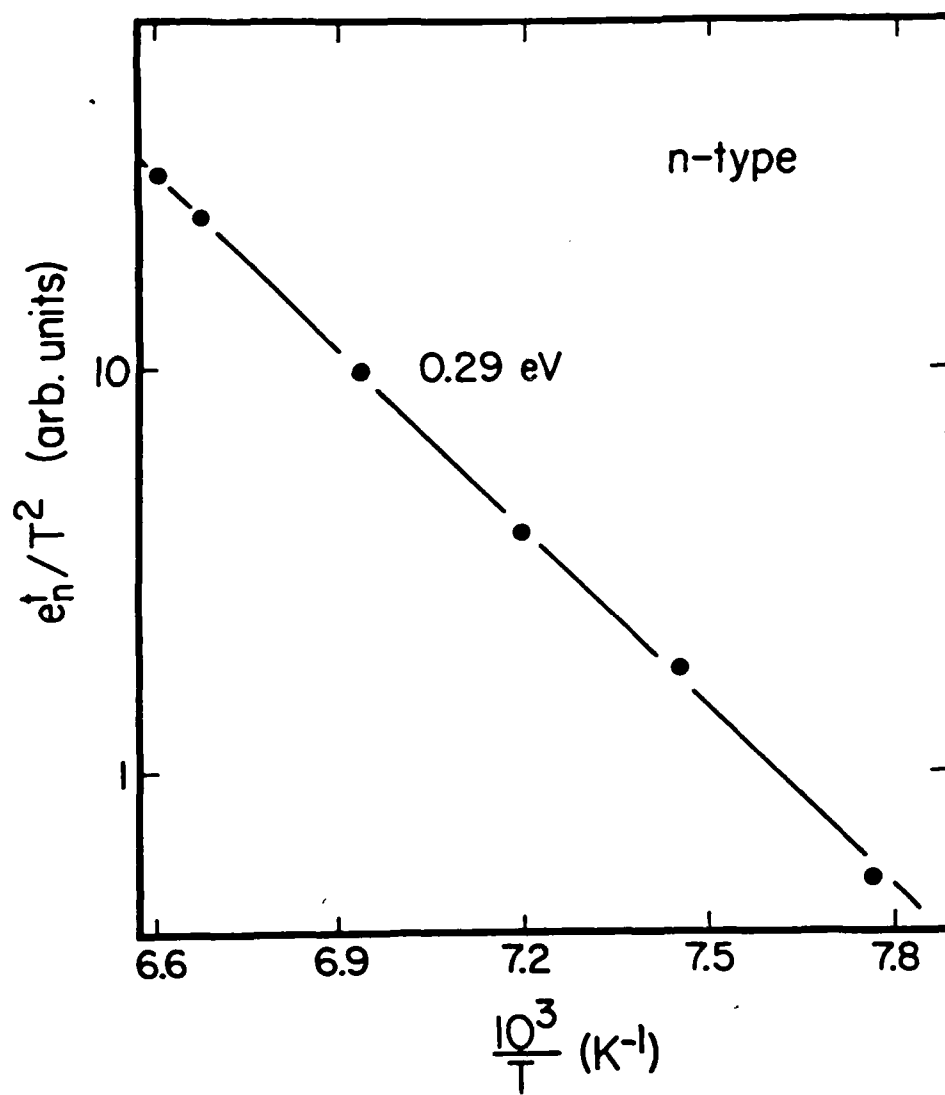


Fig. 11

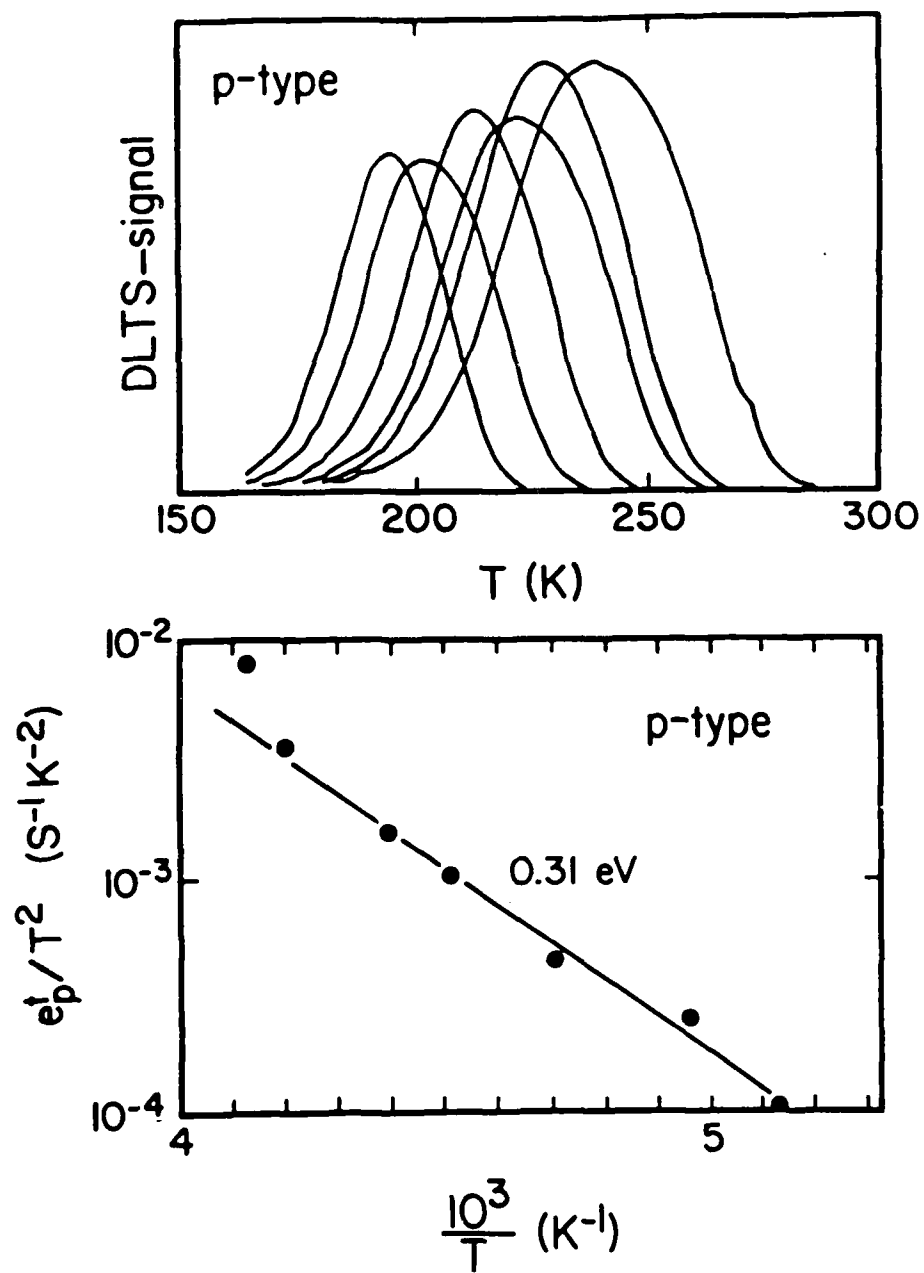


Fig. 12

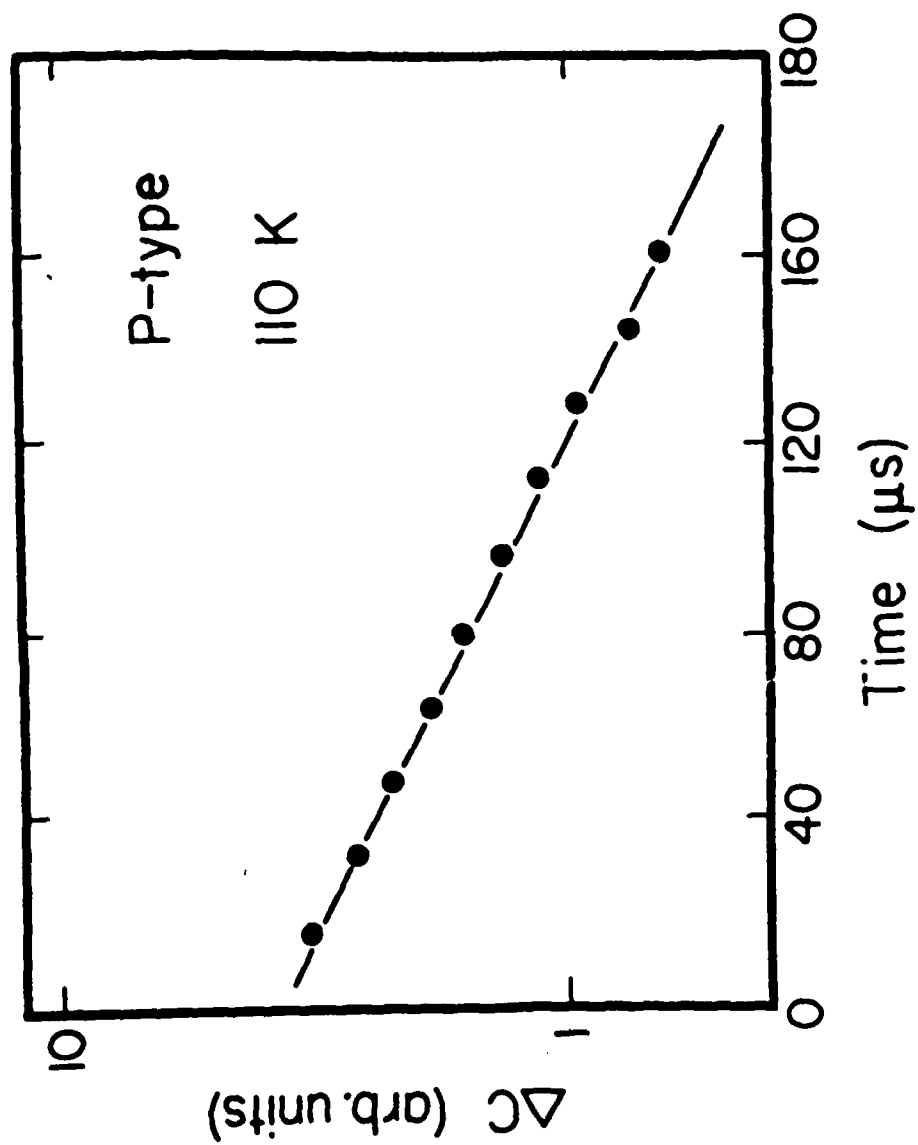


Fig. 13

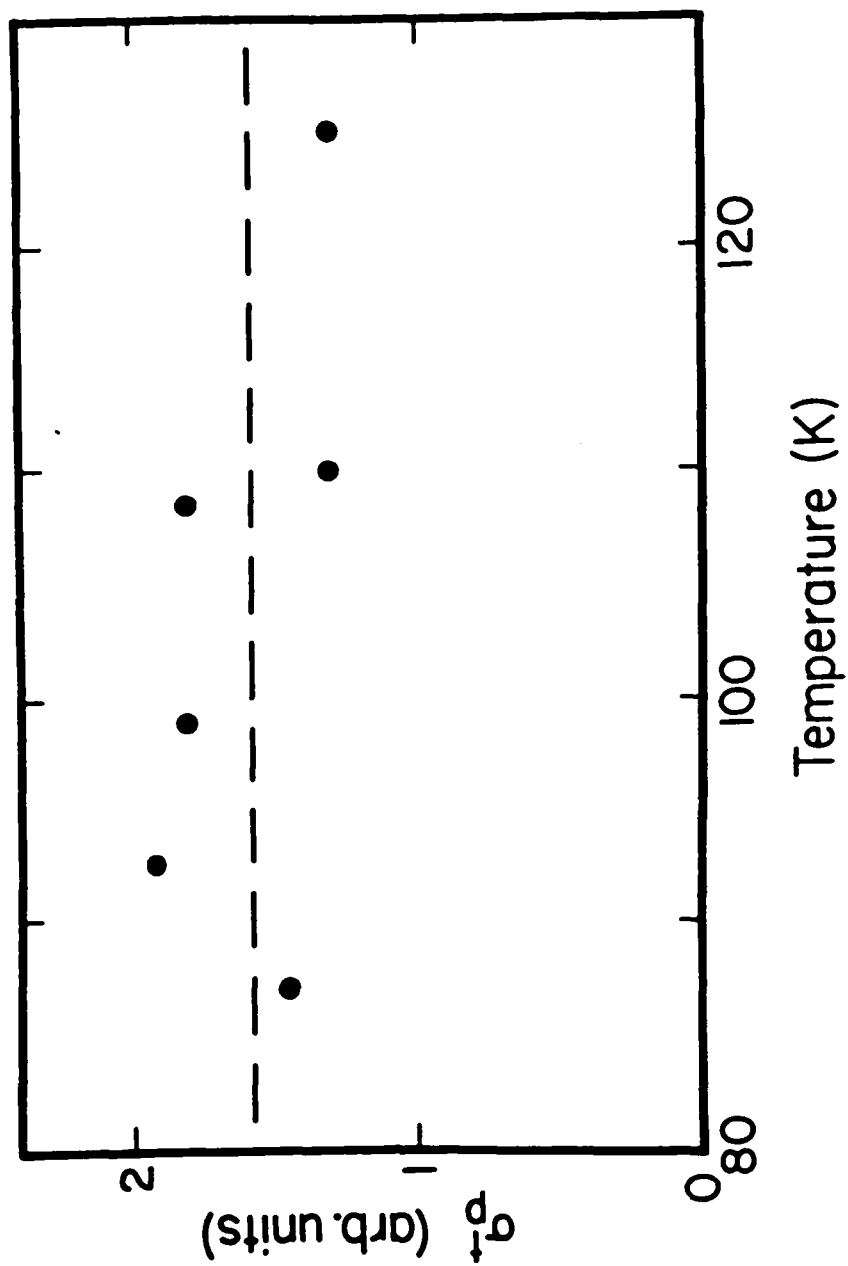


Fig. 14

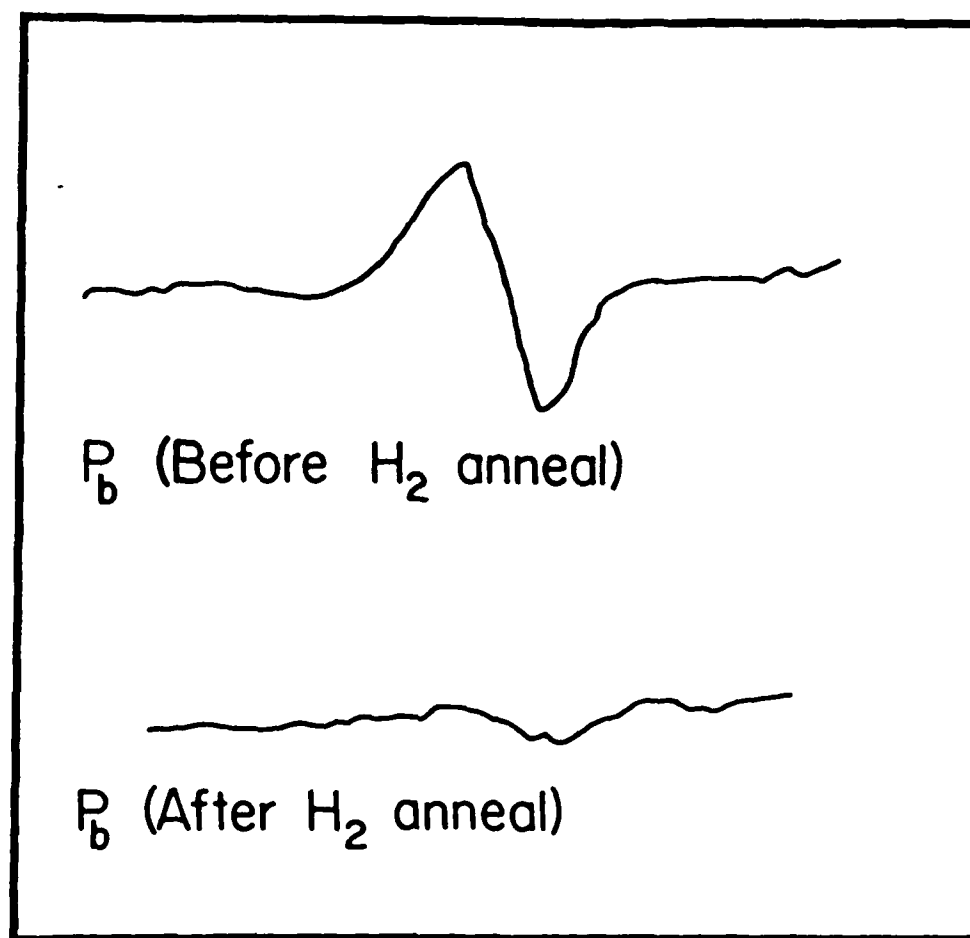


Fig. 15

- 38 -

RESEARCH REPORT

PART II

Optical Characterization of Metastable Defects in GaAs

DLTS experiments performed on Schottky contacts placed on n-type MOCVD grown GaAs, reveal the following ~~anomalous~~ behavior¹. If the sample is first heated to 400K for 15 minutes under a zero bias, two DLTS peaks with activation energies for thermal emission of electrons of 0.83eV and 0.61eV are observed. If, however, the sample is heated to 400K for 15 under a small (i.e. between -4 and -6 volt) reverse bias, two peaks are again observed, but now with activation energies for thermal emission of electrons of 0.31eV and 0.83eV. The raw DLTS peaks indicating these metastable configurations are shown in Figure 1. The 0.83eV peak is believed to be the well studied EL2 center and is not the focus of this investigation. The two remaining peaks at 0.31eV and 0.61eV, labeled M3 and M4, are thought to be one in the same defect undergoing a configurational change. Thus they are termed metastable defects, with their configurational change being temperature-induced and bias-controlled. Previous work also seems to indicate the M3 configuration to be a donor state (as determined through its bias dependent emission rate) and the M4 configuration to be an acceptor state (as determined by its lack of bias dependent emission). Isochronal anneals have also been performed on these defects and the reaction kinetics determined.¹

To further characterize these defects, the photoionization threshold energy and the photoionization cross sections were determined by measuring the change in capacitance of the sample as a function of incident light energy. If the rate of light induced capacitance change can be determined, the photoionization cross section is known via the relation²

$$e_0 = \sigma_0 \Phi$$

where σ_0 is the photoionization cross section and Φ is the light intensity. It has been shown that one only need measure the initial slope of the light induced capacitance transient to determine the relative values of the photoionization cross section. This is known as the initial slope technique for cross section determination and is more fully described elsewhere.² It is the initial slope technique which was used in this work to determine the photoionization cross section for the M3 and M4 defect centers.

The equipment used in this work was a KRATOS single grating monochrometer. The sample was held in the evacuated, LN₂ cooled cryostat, supplied with the POLARON DLTS unit which had been previously used for the electrical characterization of these defect centers. Care was taken to insure none of the optical equipment used absorbed light energy in the 0.1eV to 1.4eV range. Second order effects were eliminated through the use of order sorting filters. The sample is identical to those described elsewhere¹. GaAs films grown on n⁺ substrates by MOCVD at 750°C were intentionally doped with silicon to a uniform dopant concentration of $7 \times 10^{15} \text{ cm}^{-3}$. The GaAs was encapsulated with a silicon nitride layer grown insitu to reduce the possibility of As outdiffusion from the surface during subsequent processing. To facilitate electrical contact, the back surface was coated with an Au-Ge film and alloyed to form ohmic contacts. After removal of the nitride layer, Pt electrodes were deposited on the front surface through a shadow mask to form Schottky contacts.

Cross section measurements were made by first placing the sample in one of its metastable configurations using the method as described above. The sample was cooled down to approximately 85K, and zero biased for a few seconds to fill all defects with electrons. The sample was then reverse biased to place a portion of the filled defect centers above the Fermi level. Light of various wavelengths was then used to illuminate the sample. Once the defect threshold energy was reached, a capacitance increase was observed as trapped electrons were excited to the conduction band. The initial slope of this capacitance increase was measured as a function of incident light energy. The entire capacitance transient at 0.9eV was obtained, and the absolute value of the capacitance transient rate determined, in order to fix the absolute value of the photoionization cross section.

The results of these measurements are shown in Figure 2. As can be seen, the M3 configuration gives a threshold energy of 0.55eV and the M4 configuration a threshold of 0.3eV in good correlation with the electrical DLTS data. The absolute value for the photoionization cross section in both configurations at an energy of 0.7eV is about $1 \times 10^{-18} \text{ cm}^3$. The threshold energies seen at 0.8eV and 1.0eV are believed to be associated with the EL2 center also observed in this sample.

The photoionization threshold energies and the photoionization cross sections have been determined for a metastable defect center found in MOCVD grown GaAs. This is the first observation of a metastable system being observed using photocapacitance techniques and is shown to be an effective tool for the characterization of metastable systems.

Figure Captions

Figure 1: DLTS spectra for Schottky barrier diodes on n-type, as grown MOCVD GaAs after selected bias-temperature anneals.

Figure 2: Photoionization cross sections as determined via the initial slope technique for n-type, as grown, MOCVD GaAs, after preheating the sample to 400K for 15 minutes under a -4V reverse bias. The measurement was performed at 85K.

Figure 3: Photoionization cross sections as determined via the initial slope technique for n-type, as grown, MOCVD GaAs, after preheating the sample to 400K for 15 minutes under a 0V reverse bias. The measurement was performed at 85K.

References

1. W. Buchwald, N.M. Johnson, and L. Trombetta, App. Phys. Lett. 50, 1007, (1987)
2. H.G. Grimmeiss and B. Skarstam, Phys. Rev. B 23, 1947 (1981)

FIGURE 1

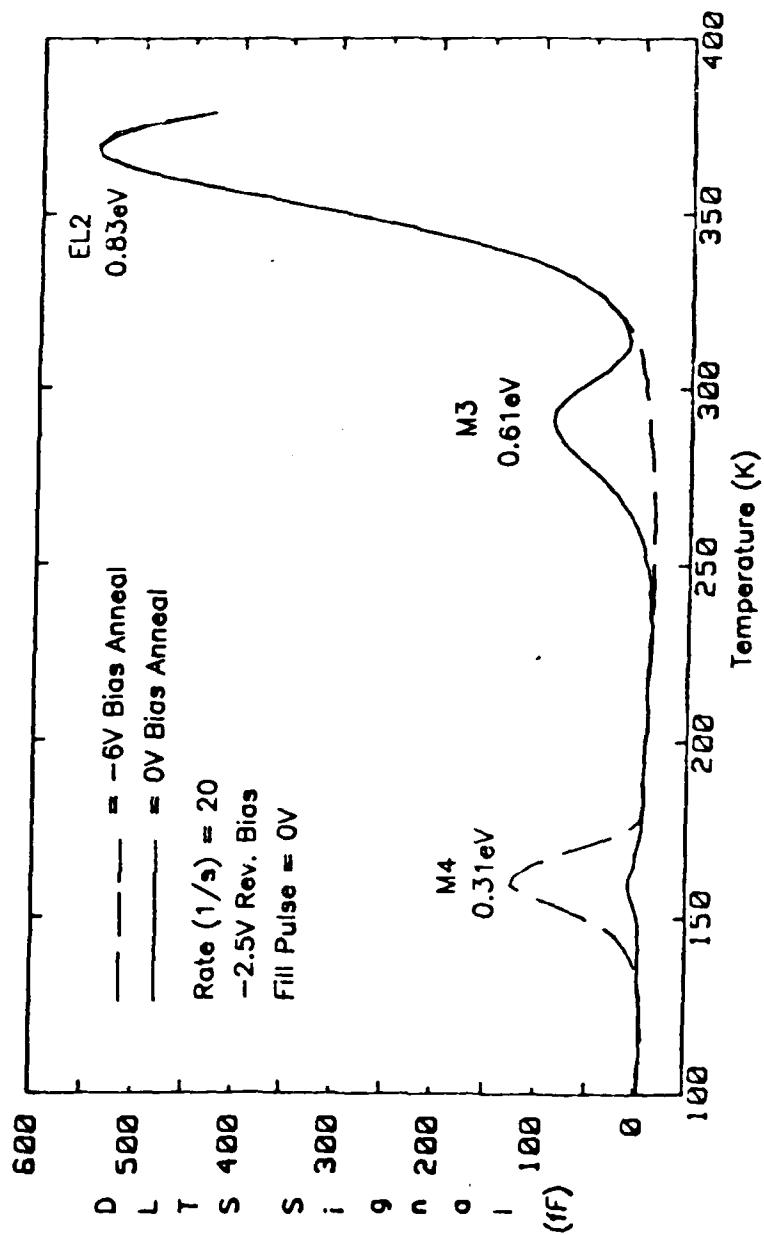


FIGURE 2

Photo Cross Sec. (M4)

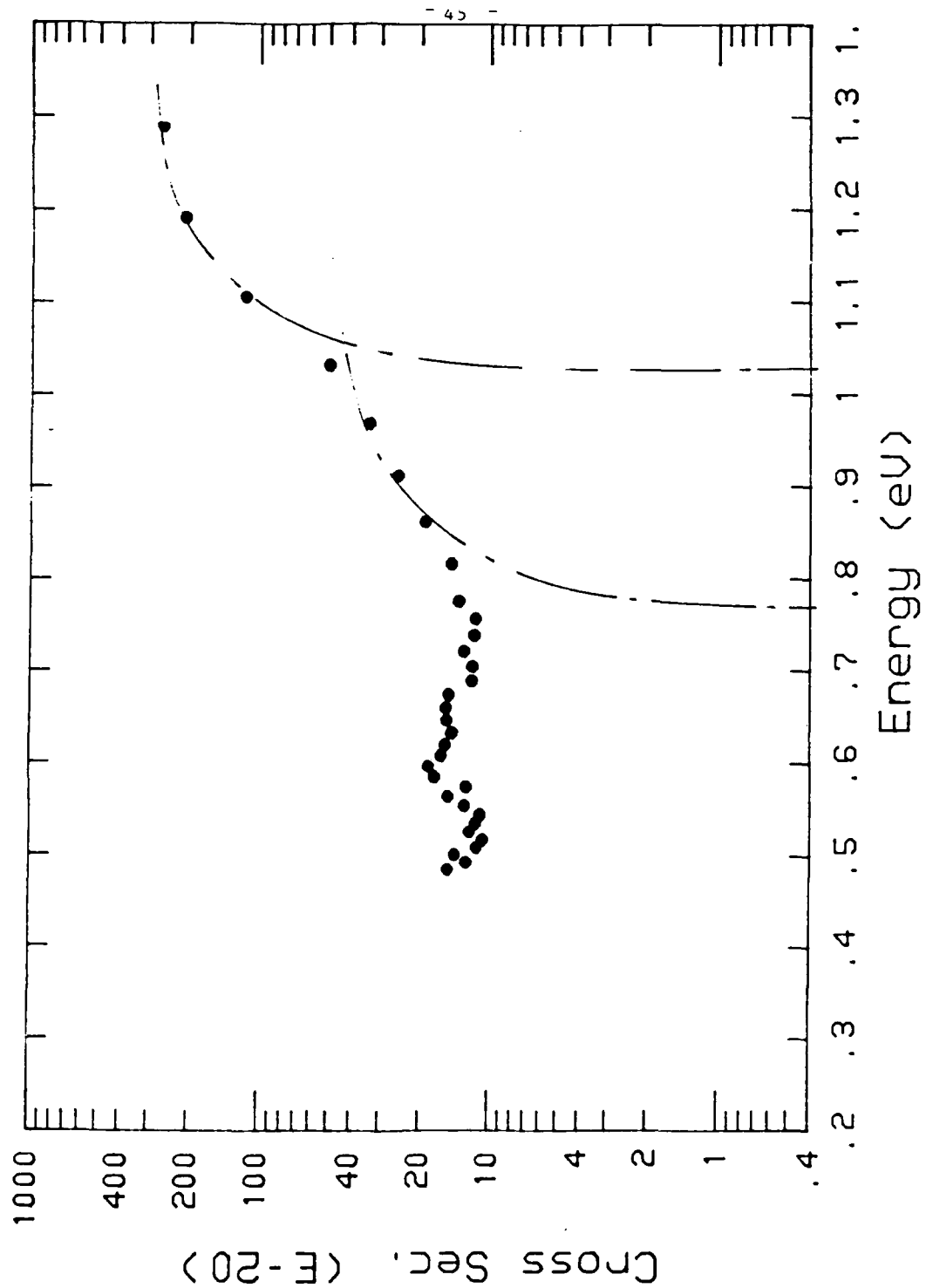
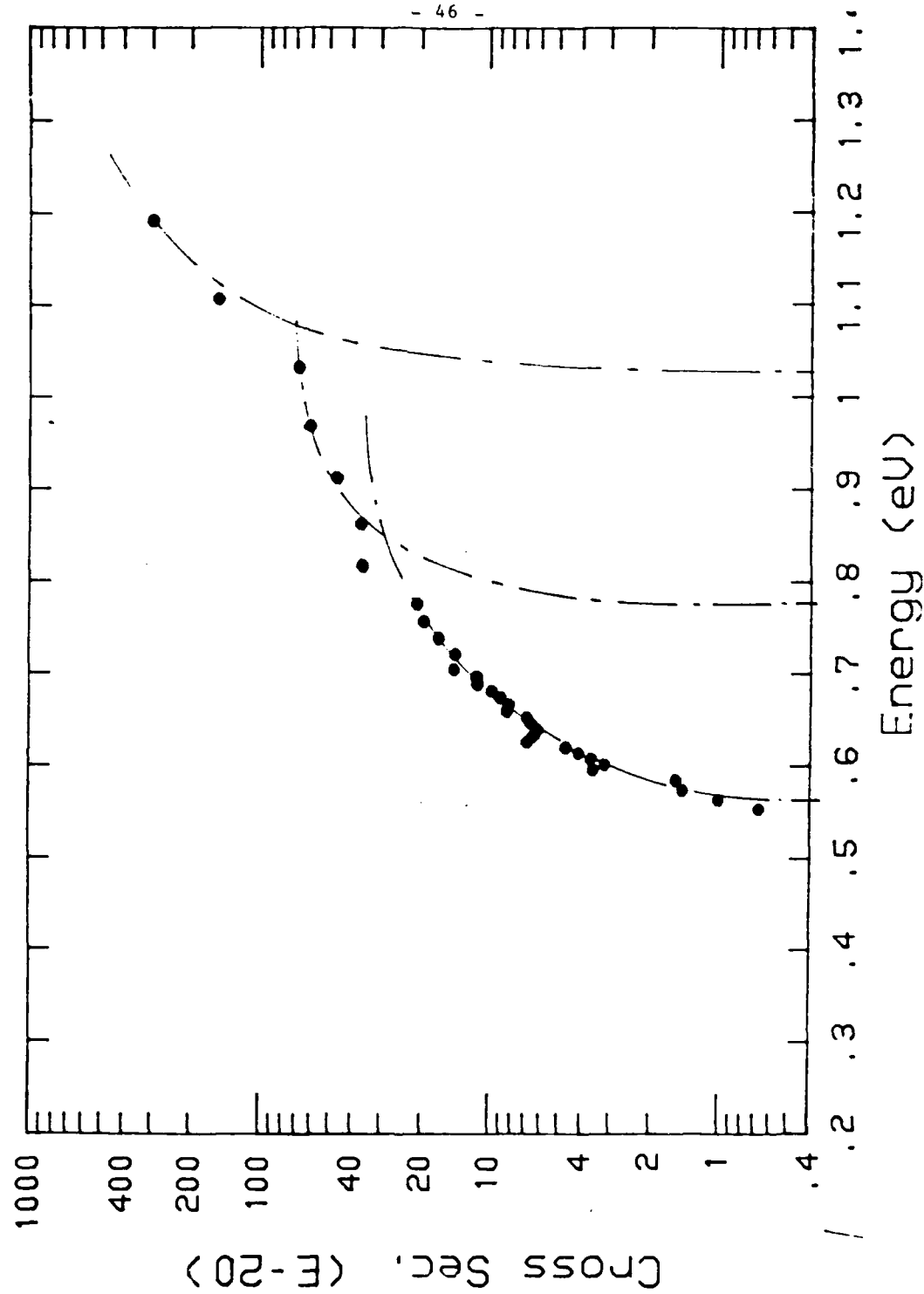


FIGURE 3

Phot. Cross Sec. (M3)



RESEARCH REPORT

PART III

**Electron Paramagnetic Resonance studies on superconducting
YBa₂Cu₃O_{7-δ} and related non-superconducting phases**

Introduction

Until recently the compound with the highest known superconducting transition, 92K, was the oxygen deficient orthorhombic perovskite $\text{YBa}_2\text{Cu}_3\text{O}_{7-\delta}$. The compound shows two interesting structural features. When viewed along the z-axis of the unit cell two planes of CuO bisected by a yttrium atom are seen. The oxygens in these layers are puckered away from the yttrium. The copper atoms at this site are labelled Cu(II). Above and below the planes lie barium atoms which separate the plane copper site from the Cu(I) site. As the oxygen deficiency increases it is the oxygen atoms within the Cu(I) plane that become disordered. This leads to the formation of linear chains of CuO extending along the b-axis of the structure, see Fig. 1. There is an associated reduction in the copper site coordination from square pyramidal to square planar.

With $\delta=0$ the oxygens in the region of the Cu(I) sites become fully disordered in ab-plane so the chains are well defined. Simple chemistry would suggest a distribution of 75% Cu^{2+} and 25% Cu^{3+} for the copper valance. For $.15 < \delta < .3$ the structure becomes a 90K superconductor. For $\delta=6.5$ all the sites should be divalent and the structure is on the verge of a transition to tetragonal symmetry.

The ion Cu^{2+} is an $S=1/2$ system and consequently shows an electron paramagnetic absorption in the free spin $g=2$ region. The exact form the spectrum is dependent on the coordination, the presence of any magnetic nuclei within the compass of the electronic wavefunction, the proximity of other unpaired spins, and on the order within the sample (polycrystalline, single crystal etc).

The electron paramagnetic resonance, EPR, absorption experiment is performed by bathing the sample in a microwave frequency radiation field and sweeping an external magnetic field. The experiments presented here were carried out at 9GHz and using field sweeps in the range 0 to 0.5T. The critical fields for this superconductor have yet to be determined accurately, however, it is known that H_{c2} is on the order of, or greater than 10T and H_{c1} is on the order of $10\text{mT}^{1.2}$. The transition temperature, T_c , is 92K for this material and will be depressed at a rate $\approx 2.5\text{TK}^{-1}$. On reducing the temperature through T_c a superconducting sample will pass into the vortex, or mixed state for the duration of most normal magnetic field sweeps (0.3 ± 0.05 T) only in those were the field approaches zero will the pure superconducting state be reached. The deviation of the field

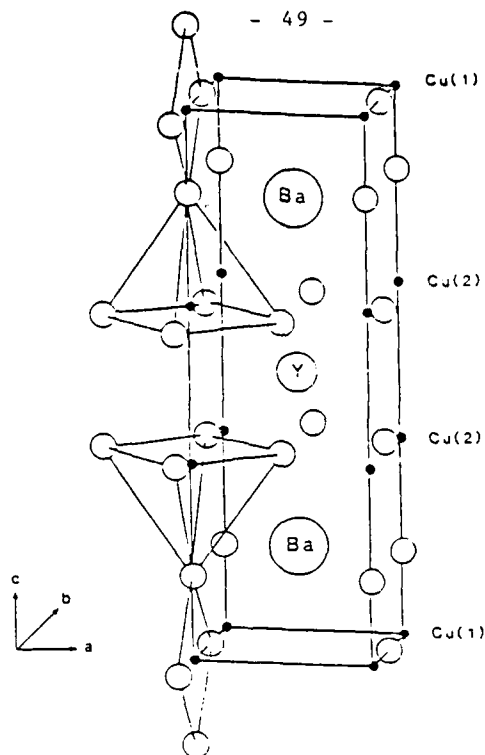


FIG. 1

The structure of $YBa_2Cu_3O_{7-\delta}$

within the sample to the applied field value is of importance. For normal sweeps this should be less than the H_{c1} value. On passing into the superconducting state the other parameter of importance is the depth of penetration of the microwave radiation field. This should reduce restricting the sample volume available; it is thought to be of the order of 1000\AA at 30K in these materials^{14,20}. In the normal state, from dc electrical conductivity data²², the skin depth at 9.5GHz is estimated to be $6\mu\text{m}$ in the a-b plane and $30\mu\text{m}$ along the c-axis hence specimens of comparable dimension will be fully bathed by the microwave radiation field, at least at temperatures above T_c .

The EPR absorption spectroscopy was performed on a Varian E109 spectrometer fitted with an Air Products variable temperature cryostat. This allowed control from room temperature to 4.2K. The samples were placed in a narrow bore (1.5mm) tube to minimise coupling to the cavity electric field. Care was taken to ensure the cavity and sample arrangement did not contribute a background resonance within the field range of interest.

EPR Studies of polycrystalline $\text{YBa}_2\text{Cu}_3\text{O}_{7-y}$

Spectra were recorded as a function of temperature. This was reduced from 290K to 70K. These measurements are presented in Fig. 2. The Zeeman magnetic field was swept from 0 to 0.4T. A resonant absorption is seen at the Zeeman magnetic field equivalent to $g \approx 2.0$. No qualitative change is seen in this absorption as a function of temperature. The spectrum is characteristic of a random array of divalent copper ions. Fig. 2 also shows the onset of a low field non-resonant absorption concurrent with the transition to the superconducting state. The intensity of this feature is greatly increased on depressing the temperature below T_c . Another characteristic feature is the increase in noise. This quickly became severe and made recording at lower temperatures difficult.

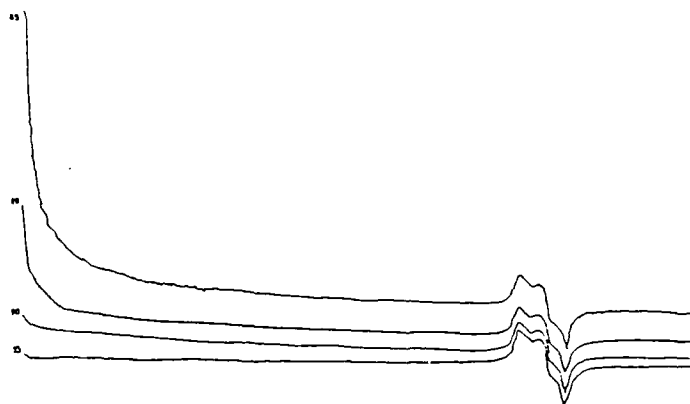


FIG.2.

EPR absorption spectra recorded as a function of temperature.

A detailed examination of the resonant absorption in the region of $g=2.0$ was carried out. The signal was recorded using a 100mT sweep and is presented in Fig. 3. Nuclear hyperfine splitting structure is resolved on this resonance though the intensity is weak and the pattern of splitting complex, it however reproducible. In an attempt to quantify this structure the absorption was scanned at a higher gain setting and using narrower field sweeps, Fig. 4.

These results are in agreement with previous EPR, absorption spectroscopy studies carried out on powdered specimens of superconducting $\text{YBa}_2\text{Cu}_3\text{O}_{7-\delta}$. A single resonance absorption line having an asymmetric shape which is attributed to divalent copper³⁻¹³ and a relatively strong non-resonant absorption which occurs, at low magnetic fields, upon cooling the material to temperatures below T_c , the superconducting transition temperature^{1,11,15-20}. A number of investigators have reported evidence suggesting that the signal attributed to the divalent copper is very likely due to an occluded non-superconducting impurity phase³⁻⁶. The intensity of the resonance absorption signal is characteristically weak in specimens exhibiting good superconducting properties. Very recently, a study of the single crystals of the superconductor $\text{YBa}_2\text{Cu}_3\text{O}_{7-\delta}$ has been carried out in the 10GHz-band region which reached similar conclusions regarding the origin of the resonance absorption¹⁴.

The onset of low field non-resonant absorption at temperatures below T_c is a pronounced effect correlated with superconductivity^{1,11,15}. It has been suggested that this absorption may be a consequence of one or more of the following: (i) a transition from the Meissner state to the mixed state¹⁵, (ii) an intragrain flux slippage characteristic of a glassy state¹⁶, or (iii) an intergrain Josephson junction effect¹⁷⁻¹⁹.

That very little, if any, EPR signal due to copper is observed in the superconducting phase is a cause for some speculation. The chemical composition of this material suggests that most of the copper is in the divalent state. Thus, broadening of the resonance absorption lines should occur as a consequence of interactions of ions of like electronic spin states. The root-mean-squared value of the fluctuating internal magnetic field was calculated to be of the order of 70mT and 90mT at the two inequivalent crystallographic copper ion sites Cu(I) and Cu(II), respectively. Such spectral linewidths attributable to copper have not been observed in this investigation, see Fig. 1. This could be taken as a basis for suggesting that exchange effects may be operating to cause spectral line narrowing. However, the asymmetry of the observed spectral line would tend to suggest such an explanation may not apply. Finally, the lack of a detected copper signal attributable to the superconducting phase could be assumed to be a consequence of spin density delocalisation or of spin-spin correlations.

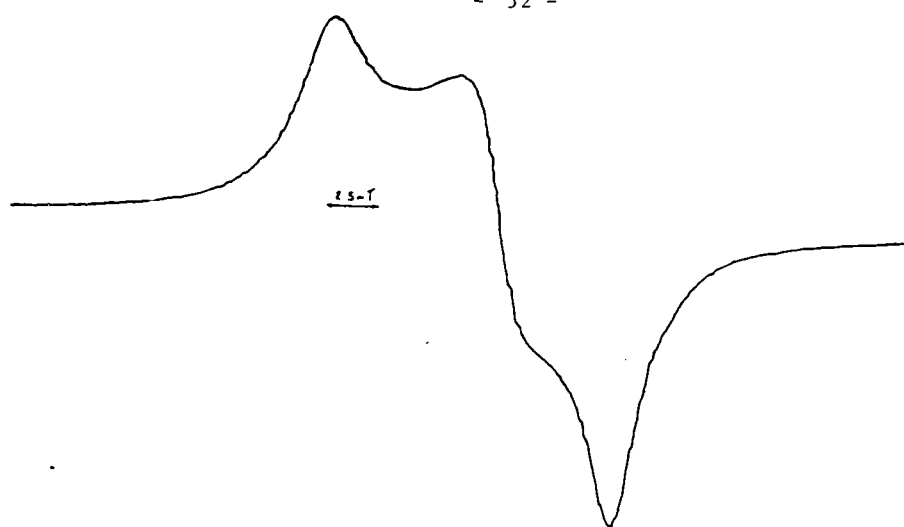


FIG. 3.

EPR absorption spectrum from powdered $YBa_2Cu_3O_{7-\delta}$ in the field region equivalent to $g \approx 2.0$.

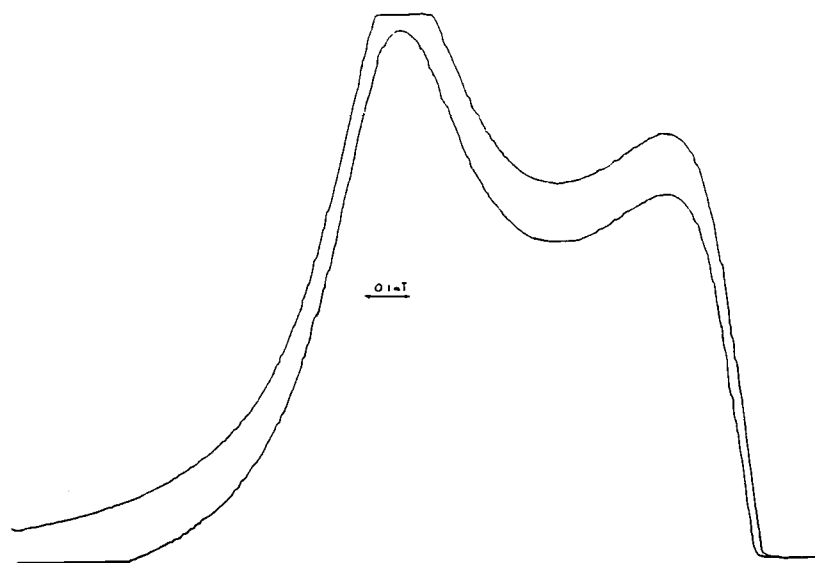


FIG. 4.

40mT field sweep of the absorption shown in FIG. 3.

Despite the strong evidence to support the association of the copper resonance with an impurity phase occlusion (also see Fig. 5). The observation of the nuclear hyperfine structure upon the absorption is of interest on three counts. Firstly, it is further evidence that this signal is not the result of exchange narrowing of intrinsic copper sites although the asymmetric shape implies that the size of the exchange term is less than the g-value anisotropy the observation of structure with a linewidth of 0.6mT further restricts this. It would clearly be impossible to account for narrowing of linewidths on the order of those quoted in the previous paragraph. Additionally, if such structure can be found in the EPR absorptions of the chemically pure impurity materials $\text{Y}_2\text{Cu}_2\text{O}_5$, Y_2BaCuO_5 , and Ba_2CuO_2 then this could help to identify local divalent copper environment in these compounds and allow comparison to be drawn with the closely related superconducting phase. This would also allow a quick and accurate identification of the dominant impurity as the hyperfine structure would act as a unique finger print to a particular impurity phase.

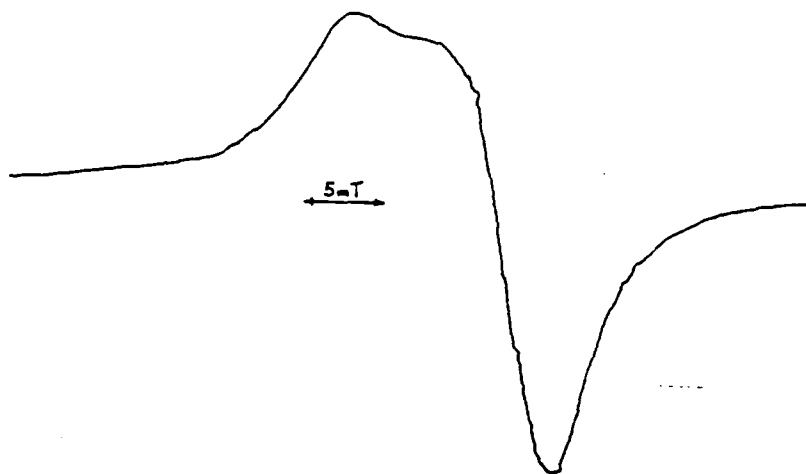


FIG. 5.
EPR absorption spectrum of Y_2BaCuO_5 recorded at 50K.

EPR Studies on $\text{Y}_2\text{BaCu}_3\text{O}_5$

It had been reported²⁴ that the phase $\text{Y}_2\text{Cu}_2\text{O}_5$ undergoes an antiferromagnetic ordering in the region of 30K. It was decided to investigate the possibility of a similar transition occurring in this phase.

The results were taken using a similar procedure, and instrumentation, to the previous study. The temperature was varied from 294K to 5K. The spectrum shown in Fig.4 was found to decay and loss of the divalent copper resonant absorption at 17K. Such a loss would be consistent with magnetic ordering.

Concluding Remarks

No EPR absorption from copper intrinsic to the superconducting phase of $\text{YBa}_2\text{Cu}_3\text{O}_{7-\delta}$ has been observed. The resonant absorption attributed to divalent copper is due to impurity phases introduced in the materials processing. The non-resonant low field absorption builds in as the temperature is depressed below T_c . Its intensity is correlated with superconduction but caution should be exercised as the role of particle size has not been fully investigated.

Work is required to identify the origin of the nuclear hyperfine structure observed on the divalent copper resonant absorption. This would involve similar studies on the three major contaminant phases. This may yield a precise diagnostic to the impurity phases present. The circumstances are particularly favourable as the pure material is EPR silent yet the major impurities introduced in materials processing are paramagnetic. It should be noted that EPR is a highly sensitive technique and would allow the detection of on the order of 10^{-8}g of paramagnetic phase. This in combination with the ability to check for superconduction and obtain an estimate of the transition temperature means that EPR may be an extremely valuable and convenient aid to materials processing. It is applicable to powdered, bulk compressed powder, and thin film specimens.

The observation of the loss of EPR absorption at 17K in the phase Y_2BaCuO_5 is consistent with the onset of magnetic ordering. This is part of a study on the EPR and magnetic properties of the related non-superconducting phases. Similar measurements are required on $\text{Y}_2\text{Cu}_2\text{O}_5$ and the

tetragonal forms of $\text{YBa}_2\text{Cu}_3\text{O}_{7-\delta}$ ($\delta \approx 0.6$ to 1).

It should be noted that EPR may still play an important part in elucidating the properties of the superconducting phase. The introduction, at levels of a few percent, of dopant ions such as manganese¹⁴ or gadolinium would allow the technique to act as a sensitive local probe. The gadolinium would substitute for yttrium and manganese would likely replace copper. Single crystal specimens would be particularly useful as any interactions monitored by the probe would reflect the materials' symmetries.

The superconductor-semiconductor interface would be open to study if an EPR active surface defect were present.

References

1. T.R. McGuire, T.R. Dinger, P.J.P. Freitas, W.J. Gallagher, T.S. Plaskett, R.L. Sandstrom, and T.M. Shaw, Phys. Rev. B36, 4032(1987).
2. P.J.M. van Bentum, H. van Kempen, L.E.C. van de Leemput, J.A.A.J. Perenboom, L.W.M. Schreurs, and P.A.A. Teunissen, Phys. Rev. B36, 5279(1987).
3. R. Durny, J. Hautala, S. Ducharme, B.Lee, O.G. Symko, P.C. Taylor, D.J. Zhen, and J.A. Xu, Phys. Rev. B36, 2361 (1987).
4. G.J. Bowden, P.R. Elliston, K.T. Wan, S.X. Dou, K.E. Easterling, A. Bourdillon, C.C. Sorrell, B.A. Cornell, and F. Separovic, J. Phys. C, 20, L545.
5. D.C. Vier, S.B. Oseroff, C.T. Salling, J.F. Smyth, S. Schultz, Y. Dalichaouch, B.W. Lee, M.B. Maple, Z. Fisk, and J.D. Thompson, Phys. Rev. B36, 8888 (1987).
6. P.P. Edwards, R. Jones, D.J. Keeble and M.R. Harrison, Nature (to be published).
7. R. Bartucci, E. Colavita, L. Sportelli, G. Balestrino, and S. Barbanera, Phys. Rev. B37, 2313 (1988).
8. K. Kojima, K. Ohbayashi, M. Udagawa, and T. Hihara, Japn. J. Appl. Phys. 26, L766 (1987).
9. F. Mehran, S.E. Barnes, T.R. McGuire, W.J. Gallagher, R.L. Sandstrom, T.R. Dinger, and

D.A. Chance, Phys. Rev. B36, 740 (1987).

10. J.H. Castilho, P.A. Venegas, G.E. Barberis, C. Rettori, R.F. Jardim, S. Gama, D. Davidov, and I. Felner, Solid St. Commun. 64, 1043 (1987).

11. P.P. Edwards, D.J. Keeble, R. Jones, and M.R. Harrison, Nature (to be published).

12. K.N. Shrivastava, J. Phys. C. 20, L789 (1987).

13. M.D. Sastry, A.G.I. Dalvi, Y. Babu, R.M. Kadam, J.V. Yakhmi, and R.M. Iyer, Nature 330, 49 (1987).

14. S.M. Marshall, D.J. Keeble, J.P. Rice, and D.M. Ginsberg, Phys. Rev. B (Submitted)

15. C. Rettori, D. Davidov, I. Belaish, and I. Felner, Phys. Rev. B36, 4028 (1987).

16. K.W. Blazey, K.A. Muller, J.G. Bednorz, W. Berlinger, G. Amoretti, E. Buluggiu, A. Vera, and F.C. Matarotta, Phys. Rev. B36, 7241 (1987).

17. S.V. Bhat, P. Ganguly, T.V. Ramakrishnan, and C.N.R. Rao, J. Phys. C. 20, L559 (1987).

18. J. Stankowski, P.K. Kahol, N.S. Dalal, and J.S. Moodera, Phys. Rev. B36, 7126 (1987).

19. K. Khachatryan, E.R. Weber, P. Tejedor, A.M. Stacy, and A.M. Portis, Phys. Rev. B36, 8309 (1987).

20. S.H. Glarum, J.H. Marshall, and L.F. Schneemeyer, Phys. Rev. B, (to be published)

21. M. Beno, L. Soderholm, D.W. Capone II, D.G. Hinks, J.D. Jorgensen, J.D. Grace, I.K. Schuller, C.U. Segre, and K. Zang, Appl. Phys. Lett. 51, 57 (1987).

22. S.W. Tozer, A.W. Kleinsasser, T. Penney, D. Kaiser, and F. Holtzberg, Phys. Rev. Lett. 59, 1768 (1987).

23. J.M. Tranquada, P. Zolliker, D.E. Cox, A.I. Goldman, H. Modden, G. Shirane, D. Vakin, S.K. Sinha, M.S. Alvarez, A.J. Jacobson, and D.C. Johnston, Proceedings of the March Meeting APS, 721 (1988).

24. R. Troc, Z. Bukowski, R. Horyn, and J. Klamut, Phys. Lett. A 125, 222 (1987).

END

DATE
FILMED

10 - 88